Level 3 Feature based Fingerprint Identification

Satyabrata Swain

Department of Computer Science and Engineering
National Institute of Technology Rourkela
Rourkela-769 008, Odisha, India

Level 3 Feature Based Fingerprint Identification

Thesis submitted in partial fulfillment
of the requirements for the degree of

Master of Technology

(Research)

in

Computer Science and Engineering

by

Satyabrata Swain

(Roll: 612CS102)

under the guidance of

Prof. Banshidhar Majhi

NIT Rourkela

&

Prof. Pankaj Kumar Sa

NIT Rourkela

Department of Computer Science and Engineering
National Institute of Technology Rourkela
Rourkela-769 008, Odisha, India

Department of Computer Science and Engineering
National Institute of Technology Rourkela
Rourkela-769 008, Odisha, India.

December 26, 2014

Certificate

This is to certify that the work in the thesis entitled *Level 3 Feature based Fingerprint Idenitification* by *Satyabrata Swain*, bearing roll number 612CS102, is a record of an original research work carried out under my supervision and guidance in partial fulfillment of the requirements for the award of the degree of Master of Technology (Research) in Computer Science and Engineering. Neither this thesis nor any part of it has been submitted for any degree or academic award elsewhere.

Pankaj Kumar Sa
Assistant Professor

Banshidhar Majhi
Professor

Acknowledgment

I owe deep gratitude to the ones who have contributed greatly in completion of this thesis.

Foremost, I would like to express my sincere gratitude to my advisor, Prof. Banshidhar Majhi and Prof. Pankaj Kumar Sa for providing me a platform to work on challenging area of biometrics. His profound insights and attention to details have been true inspirations to my research.

I am very much indebted to Prof. Bibhudatta Sahoo, Prof. Pabitra Mohan Khilar, and Prof. Dipti Patra for providing insightful comments at different stages of thesis that were indeed thought provoking. My special thanks goes to Prof. Ratnakar Dash for contributing towards enhancing the quality of the work in shaping this thesis.

I would like to thank all my friends and lab-mates for their encouragement and understanding. Their help can never be penned with words.

Most importantly, none of this would have been possible without the love and patience of my family. My family to whom this dissertation is dedicated to, has been a constant source of love, concern, support and strength all these years. I would like to express my heart-felt gratitude to them.

Satyabrata Swain

Abstract

In this thesis, two novel schemes have been proposed: one scheme on dots and incipient ridges extraction and another scheme on matching using level 2 and level 3 features. Dots and incipient ridges are extracted by tracing valley. Starting points are found on the valley by analyzing the frequencies present in the fingerprint. Valleys are traced from the starting point using *Fast Marching Method (FMM).* An intensity based checking method is used for finding these feature points. Delaunay triangle has been constructed using level 2 feature. A novel algorithm of selecting compatible triangle pair from Delaunay triangle is proposed. A novel set of feature parameters are constructed by establishing spatial relation between minutiae and dots-and-incipient. Pore based matching has been performed using *Robust Affine Iterative Closest Point algorithm.* These extended features (dots, incipient ridges, and pores) are helpful for forensic experts. However, forensic experts deal with full-to-partial print matching of latent fingerprint. Hence, Full-to-partial fingerprint matching has been carried out. Partial print is constructed by cropping a window from a full fingerprint in two ways such as, non-overlapped cropping and random cropping. Form the experiment, it has been observed that random cropping based fingerprint has better accuracy than non-overlapped cropping. For performance evaluation of the proposed algorithm, two public databases have been used: NIST SD30 database and IIIT Delhi rural database. All images in SD30 are taken in constrained environment and images in IIIT database are taken in unconstrained environment. Feature level and score level fusion have been carried out for fusing different levels of feature. It has been observed that score level fusion shows better accuracy than feature level fusion.

Keywords: fingerprint, extended feature, dots and incipient ridges, level 3 feature, delaunay triangle, fast marching method.

Contents

List of Figures

List of Tables

Chapter 1

Introduction

Biometric identification provides a trustable solution to the problems faced by conventional authentication approaches. Biometrics are categorized into two types such as physiological and behavioral. Physiological biometrics is based on measurements and data that derived from direct measurement of a part of the human body. Iris, fingerprint, palmprint, and face are examples of leading physiological biometrics. On the other hand, behavioral characteristics is a form of action taken by a human being. Behavioral biometrics is computed from the measurements and the data that is derived from the corresponding behavioral characteristics. Signature, voice recognition, and keystroke dynamics are examples of leading behavioral biometric traits. Biometric identifiers for personal authentication reduce or eliminate reliance on tokens, PINs, and passwords. Various modes of authentication are shown in Figure 1.1. The primary advantage of biometrics over token-based and knowledge-based approaches is that, it cannot be misplaced, forgotten or stolen. The characteristics are distinct and can identify authorized persons. It is very difficult to spoof biometric systems as the person to be authenticated must present physically. The use of a biometric system for recognition purpose requires following characteristics.

- *Distinctiveness*: Any two persons should be sufficiently different in terms of the attributes.

- *Universality* : Each person should poss the attributes. The attribute must be one that is universal and should not lose in any accident and disease.

- *Collectability* : The attributes should be measured quantitatively.

- *Permanence* : The attributes should be sufficiently invariant over a period of time.

- *Reducibility* : The captured data should be capable of being reduced to a file which is easy to handle.

- *Inimitable* : The attribute must be irreproducible by other means. The less reproducible the attribute, the more likely it will be authoritative.
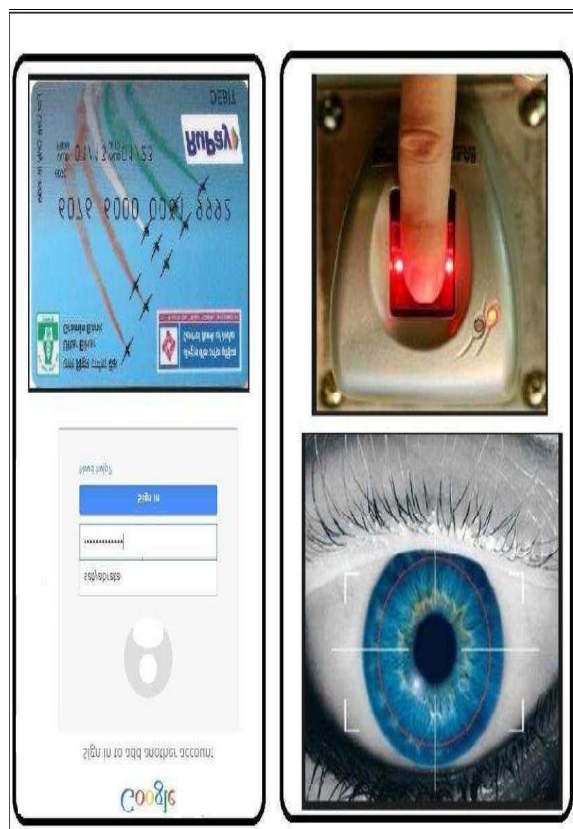
Figure 1.1: Various forms of authentication. Left: Traditional methods of authentication using token based and knowledge based approaches. Right: Use of biometrics to claim identity.

Each biometric has its own strength and weakness, and choice of a particular biometric typically depends upon the requirement of the application. Biometric researchers have classified the characteristics of a biometric trait into three levels such as high, medium, and low. Level of characteristics of all biometric traits has

been described in Table 1.1. A biometric trait is chosen depending on the level of characteristics it has. In 1880, Henry Faulds and William James Herschel explained the uniqueness and permanence of fingerprint [1]. Consequently, English scientist Sir Francis Galton proved that, there are 64 billion different fingerprints can be possible [1]. Due to the property of uniqueness and persistence, fingerprints are most widely used biometric. One researcher stated that "two twins may have chance of same DNA but different fingerprints" [2]. Skin on human fingertips contains ridges and valleys (furrows) which together form distinctive patterns. These patterns are fully developed in the womb and are permanent throughout the lifetime. Prints of those patterns are called as fingerprints. Fingerprints have been routinely used by the forensics community for over one hundred years and automatic fingerprint identification system over fifty years. According to biometric market report by International Biometric Group [1], "fingerprint based biometric has more than fifty percent of market share among all the biometric technology".

A biometric system is essentially a pattern recognition system that operates in three steps. First, collect biometric data from an individual using sensor. Second, features are extracted from the acquired data. Third, authentication of an individual based on the result of comparison of the feature set against the template set in the database [2, 3]. An important issue to be considered while designing a biometric system is how a person is recognized. Based on the application context a biometric system operates in two different modes [3]. In *verification* mode, the system validates a candidate's identity by comparing the captured biometric data with his own biometric template stored in the database. In such a system, a person who desires to be recognized claims an identity, usually via a PIN, a username, a smart card, etc. One-to-one comparison is carried out by the system to know whether the identity claimed by an individual is genuine or not. In *identification* mode, the system searches the entire database to find the identity of a person. Therefore, the system conducts a one-to-many comparisons to establish candidate's identity. The diagrammatic representation of verification and identification are given in Figure 1.2. Applications of biometrics include sharing networked computer resources, granting

Table 1.1: Comparison of different biometric traits based on their characteristics, H: High, M: Medium, L: Low

Biometric Identifier	Universality	Uniqueness	Permanence	Collectability	Performance	Acceptability	Circumvention
Fingerprint	M	H	H	M	H	M	M
Face	H	L	M	H	L	H	L
Facial thermogram	H	H	L	H	M	H	L
DNA	H	H	H	L	H	L	L
Ear	M	M	H	M	M	H	M
Gait	M	L	L	M	L	H	M
Hand geometry	M	M	M	H	M	M	M
Hand vein	M	M	M	M	M	M	L
Iris	H	H	H	M	H	L	L
Keystroke	L	L	L	M	L	M	M
Odor	H	H	H	L	L	M	L
Retina	H	H	M	L	H	L	L
Signature	L	L	L	M	L	H	H
Voice	M	L	L	M	L	H	H

access to nuclear facilities, performing remote financial transactions or boarding a commercial flight.
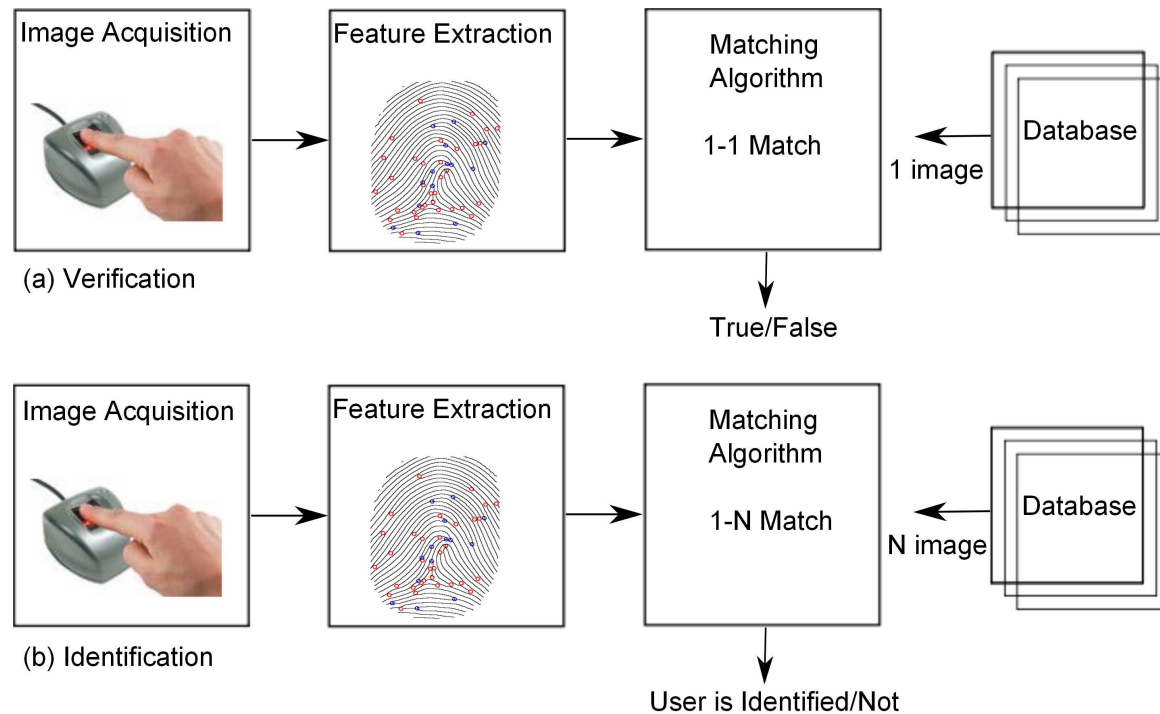
Figure 1.2: Different modes of biometric recognition

Biometrics such as signatures, iris, voice, and retinal blood vessel patterns all have significant drawbacks. Although signatures are cheap and easy to obtain and store, they are impossible to identify automatically with assurance, and can be easily forged. Electronically recorded voice is susceptible to changes in a person's voice, and they can be counterfeited. Sensor of iris is more expensive. On the other hand, fingerprint is unique, permanence, and its sensors are cheaply available that make it a suitable biometric trait for identification. In this thesis, we have investigated different levels of features of fingerprint, its extraction and matching techniques used in both automatic fingerprint identification system (AFIS) and forensic examiner (for criminal detection). Before going to the description on fingerprint matching system, it is important to know the formation and anatomy of fingerprint.

1.1   Formation and Anatomy of Fingerprint

With the interaction of a particular genotype and environment, a phenotype can be uniquely identified. Fingerprint is considered as a phenotype. When the fingertip starts to differentiate, fingerprint is visible to the tips. This differentiation process is elicited by the growth of the volar pads on the fingers, soles, palms, and toes. During the differentiation process, the flow of amniotic fluids around the fetus and its position in the uterus changes. So the growth of the cells on the fingertips in a micro environment varies over the fingertips. There are many variations during the formation of fingerprint, which makes it identical to individual. Fingerprint is not only identical but also permanent. Finger skin consists of three anatomical layers: epidermis, dermis, and hypodermis. Epidermis the outer layer of the skin acts as a receptor organ and providing a protective layer over the tissues and prevents evaporation of water. Dermis is the most vital layer which lies under epidermis and acts as a blood reservoir and temperature regulator. This layer contains connecting tissues that consist of networks of blood vessels, fibers, cells that provide structural support to the epidermis. Hypodermis lies beneath the dermis which is a loose connecting tissue act as an energy reservoir. Fibers are the links of these three layers. These three layers are shown in Figure 1.3.

1.2   Fingerprint Feature Representation

Fingerprint is produced from epidermis of fingertips when the finger is pressed over a surface. It consists of continuous pattern of ridges and valleys. Generally, width of the ridge varies from $100\mu m$ to $300\mu m$, so the period of valley or ridge is about $500\mu m$ [1]. While running parallel, sometimes ridge terminates and bifurcates, called as ridge ending and bifurcation respectively. Ridge moves at a high curvature during motion and those high curvature regions are called as singular regions or singularities or level 1 feature as shown in Figure 1.4 (a). Depending upon the shape, singularities are classified as, loop, delta, and whorl. These are represented by the symbols ∩, Δ and, O respectively. These singularities are called as a core as these are used for alignment while matching between two fingerprints. The concept of core was
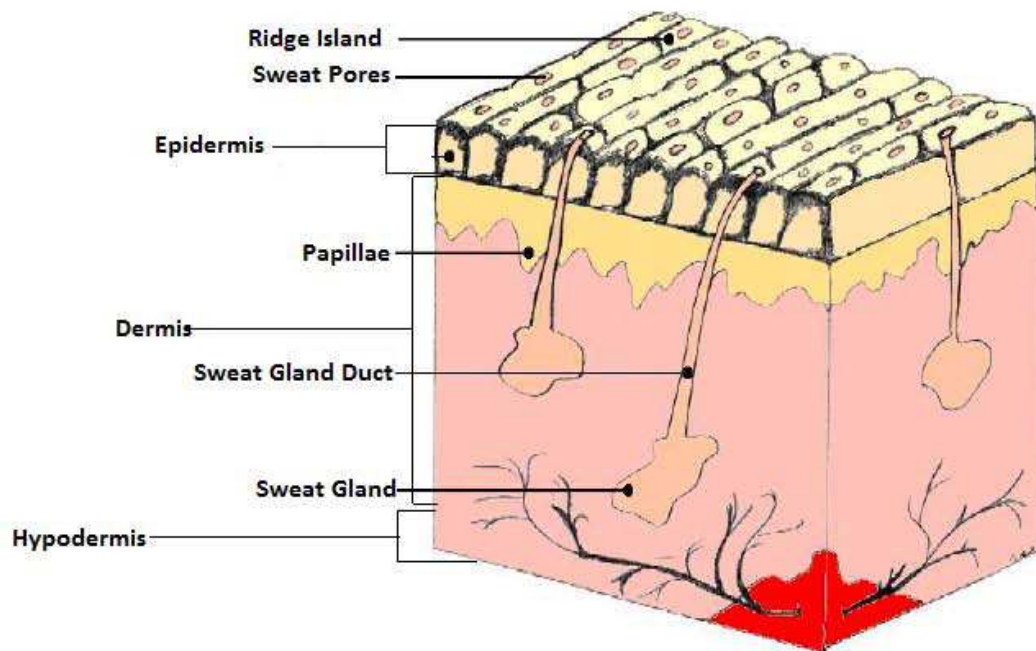
Figure 1.3: Anatomy of fingerprint

introduced by Henry and according to him, a core is the north most point of the inner most ridge line [1]. One of the important features in the fingerprint is minutiae. Minutiae mean small details, however in case of fingerprint, it is defined as the way of representation that the ridges can be discontinuous. Most popular and important minutiae are ridge ending and bifurcation (level 2 feature) as shown in Figure 1.4 (b). Sir Francis Galton was the first person who told that the distributions of minutiae on a fingerprint are unchanged over the life time of a human and are unique for each person. When a fingerprint is taken through a sensor, ridges and valleys are represented by black-and-white lines respectively. In the image negative, we will get the minutiae exactly at the same point, but positions of ridge ending and bifurcation are interchanged. So these features exhibit the property of duality. Besides these features, fingerprint contains many minute features such as pores, dots, incipient ridge, short ridges, ridge protrusions, spurs, etc. Dots, incipient ridges, and pores have been shown in Figure 1.4 (c). In this thesis extraction of two level 3 features, dots and incipient ridges have been proposed. Fingerprint identification has been proposed using both level 2 and level 3 features.

Arch   Tented   Left   Right   Double   Whorl
        Arch   Loop   Loop   Loop

(a)

Ridge Ending   Bifurcation

(b)

Dots   Incipient Ridge   Pores

(c)
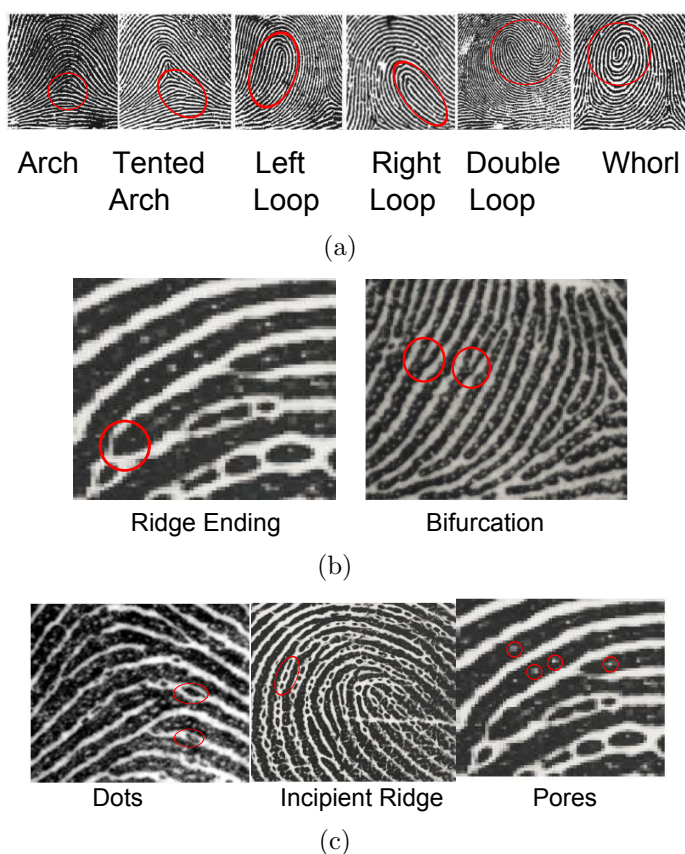
Figure 1.4: (a) Level 1 feature, (b)Level 2 feature, (c) Level 3 feature

1.3   Fingerprint Identification System

A fingerprint identification system is a pattern recognition system that gathers fingerprint image of an individual, extract the feature, and compare it against the features stored in the database. The fingerprint which claims for identity is known as a probe, and the set of fingerprints those are stored in the database are called as gallery. Generally, a fingerprint identification system consists of four modules as follows.

Fingerprint Acquisition

While using a fingerprint in the context of AFIS or forensic application, the first step is image acquisition. The fingerprint image is digitized. There is two way of doing this: off line and live scan. In the off-line system, smudging ink on the fingertips and an impression is taken on a white paper. In forensic application, an image is taken from

the spot using some chemicals, and a print made on a paper. This type of fingerprint is popularly called as latent fingerprint and is used for criminal detection. Then this paper is digitized either by a scanner or a high-quality digital camera. In live scan method, the fingerprint is taken from a sensor having a capability of converting it into the digital form. This method is adopted in AFIS.

Preprocessing

The fingerprint is separated from its background to get the Region of Interest (ROI) that means the area that is not part of the fingerprint which should be discarded. There are some parts of fingerprint, which are either full of noise or may not contain sufficient information and should be discarded. Then, some image enhancement technique is used to improve the quality of the image. Image enhancement is an important step in the fingerprint identification system, because the accuracy depends upon the quality of the fingerprint. There are different approaches of image enhancement, which will be covered in the later part of this thesis.

Feature Extraction

Features are the significant details in an image which is used to uniquely identify an image over a gallery set. The feature should be invariant over scaling, translation, and rotation. There are many mathematical models available to extract features from an image. Some feature extraction techniques are discussed in Chapter 2 and Chapter 3.

Matching

Matching finds the similarity between two feature sets. In verification mode (one to one), matcher either accept or reject the input feature of an image based on a threshold value. However, in case of identification mode (one to many), m number of score (m number of templates in gallery) is generated and the optimum score (minimum for dissimilarity based matching and maximum for similarity based matching technique) along with a threshold determines the matching template.

1.4 Various Performance Measures

When we are designing a matching algorithm for two sets of strings or numbers, the algorithm returns true when there is a perfect match. However, this type of algorithm is not applicable for biometric data, due to scanning condition (fingerprint may dry or wet), change in acquisition condition. So, two templates from same individual may not match always. The rate of difference of two images originating from same individual is called as *intra-class* variation. On the contrary, rate of difference of two images originating from different individual is called as *inter-class* variation. Degree of similarity between two images is called as a score. The score obtained from *intra-class* and *inter-class* are called as genuine score and impostor score respectively. While matching, a threshold (τ) for the score is defined, matching score above τ will be genuine score and below it, will be an impostor score. However, in practice, this is not always true and may generate an error. Various performance measures are used to evaluate a fingerprint identification system as follows.

- *False Rejection Rate (FRR)*: A false rejection occurs when an individual is not matched correctly to his/her own existing biometric template. This case arises when a genuine score falls below the threshold. FRR is the rate of rejection with respect to the individual those are correctly accepted.

- *False Acceptance Rate (FAR)*: A false acceptance occurs when an individual matched incorrectly. This case arises when an impostor score exceeds the threshold. FAR is the rate of false acceptance with respect to the individual those are correctly rejected.

- *Equal Error Rate (EER)*: Equal Error Rate is the condition where False Acceptance Rate and False Rejection Rate coincide ($FAR = FRR$). In biometric system, EER is considered as the standard for accuracy as lower the equal error rate, higher the accuracy.

- *Genuine Acceptance Rate (GAR)*: Genuine acceptance occurs when an individual correctly matched. This case arises when a genuine score exceeds

the threshold. GAR is the rate of true acceptance over the total individual. It can also be defined as,

$$GAR = 1 - FRR \tag{1.1}$$

- *Receiver Operating Characteristic (ROC)*: Using ROC curve, we are able to analyze the performance of a biometric system. It depicts the graph between FAR and GAR.
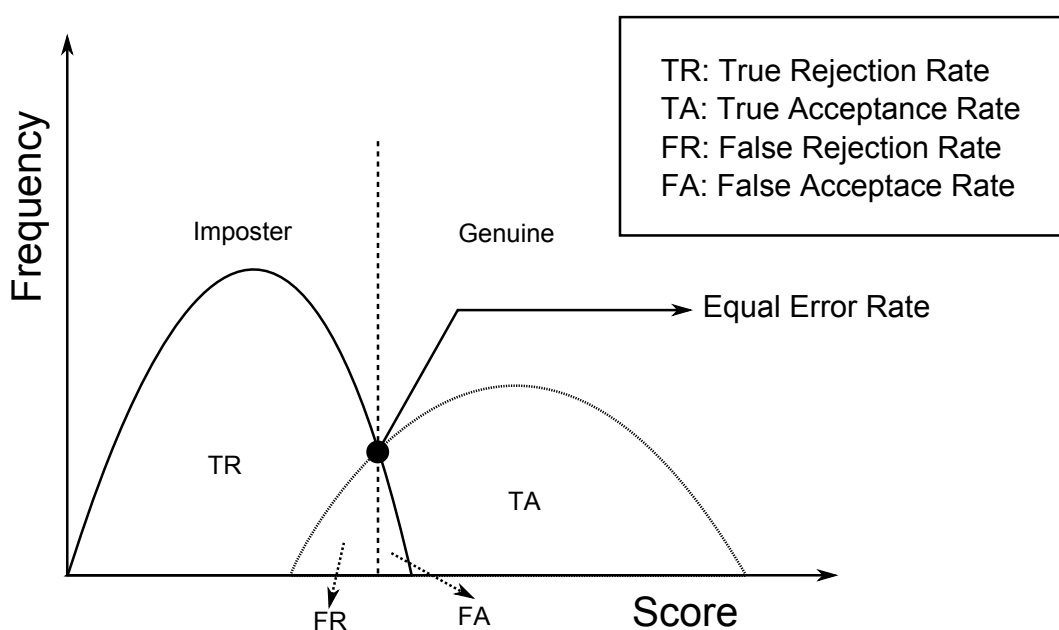
Figure 1.5: Score distribution

1.5 Fingerprint Databases used

To measure the performance of fingerprint biometric system, extensive experiments are carried out at various levels. This section discusses in detail about the databases used in experiments. Experimental results are obtained using various available datasets such as National Institute of Standards and Technology (NIST) special database 30 (SD30) [4] and Rural Indian Fingerprint Database of IIIT Delhi [5]. National Bureau of Standards (NBS) popularly known as NIST is a subdivision of Federal Bureau of Investigation (FBI) for standardization. They have relied

a series of fingerprint database for evaluating and testing different fingerprint identification algorithm. NIST designed a compressed algorithm called as Wavelet Scalar Quantization (WSQ). This WSQ became a standard for storing and exchanging the fingerprint database. SD30 also contains WSQ fingerprint images. Fingerprints are stored inside a card. Each card contains 10 fingerprints. The Database contains fingerprint scanned at 19.7 ppmm (500 ppi) and 39.4 ppmm (1000 ppi). As we are extracting level 3 feature (prominent high-resolution image), so we are using only 1000 ppi image. It consists fingerprints of 36 individuals, two impressions per individual for ten fingerprints. Rural Indian Fingerprint Database consists of 1000 ppi image collected from both urban and rural people for performance evaluation. The database contains fingerprints of 150 individuals (75 from rural and 75 from urban) of left and right index finger. Ten samples have been taken from each finger.

1.6   Literature Review

The first AFIS was developed by FBI and Paris police department [6]. The team stated that there are three steps involved in the development of an AFIS: image acquisition, ridge characteristic's extraction and pattern matching. The current technology while developing an AFIS also uses the same methodology as FBI. While image acquisition; resolution, number of pixel, geometric distortion and contract area should be taken care. US Criminal Justice Criminal Service, a part of FBI proposed a set of specification, which ensures the mentioned criteria. Although fifty years before, the first off line sensor was developed, still this technique is used by forensic export [7, 8]. First live scan sensor was designed using Frustrated Total Internal Reflection (FTIR) technique [9, 10].

Finger touches the top side of a glass prism, so ridge is on contact with prism but not the valley. Light is passed through the prism using a Light Emitting Diode (LED) and is reflected by the valleys. Valley appears as bright light where as ridge appears dark (as no reflection from the ridge). Disadvantage of this technique is geometrical distortion. An optic based distortion-free sensor is designed by Seigo *et al*. [11] using holograms. Chen *et al*. [12] proposed a small size sensor as compare to FTIR called

FTIR with sheet prism. A number of prismlet arranged side by side instead of a single prism. A smaller fingerprint sensor was proposed by Fujieda *et al*. [13] by using a fiber-optic platen. Young *et al*. [14] proposed an electro-optical based sensor which has two layers: first layer is a polymer which produces a pattern by polarizing with certain voltage, and the second layer is used to convert the fingerprint pattern into a digital form. Although the sensor size is smallest among all the existing sensor, but quality is not as good as FTIR method. Cost and size decreased drastically after the invention of solid-state technology (made from silicon). There are four ways of converting physical information into an electrical signal: capacitive, thermal, electric field and piezoelectric. In 1982 Tsikos [15] proposed a silicon based capacitive sensor which is a two-dimensional array of micro-capacitor plate embedded in a chip. When fingerprint is placed on the plate, electrical charge is created, which depends on the distance between plate and fingerprint. Charge across the ridge and valley is high and low respectively, which form a distinctive pattern. The advantage of this technique is that its performance is good with non-ideal skin condition. However, the drawback is frequently cleaning of the surface on the plate. Thermal based silicon sensor was first proposed by Edward in 1984 [16]. Temperature differentiation is created by putting a fingerprint on the sensor as ridge touches the sensor and valley maintains a distance. In order to get a well-defined feature set, the quality of the fingerprint image should be good. In practice, some noise occurs due to variation in skin and impression condition. Thus an image enhancement technique is used to reduce the noise. In 1988 O'Gorman and *et al*. [17, 18] proposed filter based fingerprint enhancement technique. He designed a filter using minimum and maximum of ridge and valley width. Sherlock *et al*. [19] proposed an enhancement technique in the frequency domain called as directional Fourier filtering. This technique is less expensive than spatial based filtering. Hong *et al*. [20] proposed a Gabor filter based enhancement technique. The benefit of Gabor filter is its frequency selection and orientation selection. Greenberg [21] designed a Gabor filter by decreasing the value of standard deviation along X-axis with respect to Y-axis. While enhancing an image with this filter is robust to noise but creates some spurious ridges.

In the earliest days, minutiae are extracted from a thinned binary fingerprint image. Crossing number is used to find the minutiae. In this method a 3×3 window is taken from the binary image. When the window contains a 1 in center and another 1 in any neighboring pixel then the central pixel is considered as ridge ending, if three 1's in neighboring pixel then it is considered as bifurcation. A large number of false minutiae are present in this method. Szekely *et al.* [22] proposed a minutiae detection technique by computing orientation image divergence. M.T. Leunga *et al.* [23] proposed a minutiae extraction technique using artificial neural network from direct gray scale image. Output of rank of a Gabor filter is given to a multilayer perceptron as input, and minutiae are obtained as output. W.F. Leung *et al.* [24] proposed a neural network based feature extraction technique using tree layer perceptron. Maio *et al.* [25] proposed minutia extraction method by tracing ridge. The pixels along the ridge have maximum gradient as compared to non-ridge pixels. Ridge tracing algorithm finds the local pixels having maximum gradient orthogonal to the ridge direction. He also proved that direct gray scale extraction reduces not only false minutiae but also processing time. Jiang *et al.* [26] proposed a minutiae extraction of variant of Maio *et al.* approach where the ridge following steps are dynamically changed according to the change of ridge contrast. Liu *et al.* [27] proposed an approach for detecting minutiae where they trace the central ridge and the two surrounding valley. Nilsson [28] *et al.* proposed minutiae detection technique using Linear Symmetry (LS) and separable Gaussian derivative filter. Minutiae are the point which lacks the symmetry that is a discontinuity of the LS vector field.

Michael Ray *et al.* [29] proposed a pore extraction technique using modified minimum squared error from a low resolution image. Anil Jain *et al.* [30] proposed a technique for extracting pore and ridge contour using wavelet transform and Gabor filter. Some authors [31] also have proposed a hierarchical matching system that utilizes the features from all three levels (level 1, level 2 and level 3) and matching are carried out using an Iterative Closest Point (ICP) algorithm. Qijun Zhao [32] proposed an adaptive pore extraction model whose parameters are changed according to the ridge direction. The image is partitioned into blocks. Parameters of a filter

are estimated for each block, and pores are detected using that filter. Malathi S *et al.* [33] proposed pore extraction using Marker controlled Watershed Segmentation for low resolution image (500 ppi). Manivanan N [34] proposed pore detection using a high pass filtering followed by correlation. Y Chen *et al.* [35] proposed a method for extracting dots and incipient ridges using wavelet transform and Gabor filters.

1.7   Motivation

Now-a-days AFIS based fingerprint identification minutiae (bifurcation and ridge ending). These feature provide promising results in full-to-full fingerprint matching due to its distinct spatial arrangement. As fingerprint has large application, one of the dominants is criminal detection (forensic application). In forensic application, a large dataset is present in the database (scanned either using live scanner or off-line scan). Forensic expert collects fingerprint images (called as latent fingerprint, collected from the surface by using some chemical) where criminal activity has happened. Then, they try to match those fingerprints against the database. The image which is taken from the spot (where criminal activity happened) is not always a full fingerprint rather than a partial print. Hence, a full to partial matching algorithm is needed. Unfortunately, most of the minutiae based matching algorithms fail to match between full to partial match, as partial print contain less number of minutiae (more than 40 minutiae is required for full to full matching algorithm but a partial print contain less than 20, however a full print contain 60-80 minutiae on average). To overcome this problem, one approach is full fingerprint reconstruction from all the partial print [36]. The disadvantage of this kind of approach is that it is expensive, and sometimes difficult to collect all fingerprint fragment to reconstruct a full fingerprint. Error like some spurious minutiae might be added in construction process. Another approach is to extract more feature from the print along with minutiae. Ashbaugh [37], a fingerprint examiner claimed that level 3 features (dots, ridge incipient, pore, protrusions, indentations, discontinuities, linear discontinuities) are unique, permanent and immutable and can be used as a feature for identification. In 2005 a committee, SWGFAST, the Scientific Working Group on Friction ridge Analysis,

Study and Technology uttered that AFIS is using less number of features. In order to improve the accuracy of AFIS, it should use all other features of fingerprint. The Committee to Define an Extended Fingerprint Feature Set (CDEFST), a committee organized by ANSI and NIST for utilizing more features in fingerprint identification which can be used in the next generation AFIS. Level 3 features are included in those category and CDEFS named these feature sets as extended feature. In the literature review, we have seen that very little work has been done on dots and ridge incipient extraction. In this thesis, we have suggested a level 3 feature based fingerprint identification system. The recognition results are compared with level 2 features.

1.8   Objectives

The objectives of this thesis work are to:

- extract level 3 features such as dots and incipient ridges from fingerprint.

- suggest a matching technique using the extracted level 3 features.

- use different levels of fusion techniques for fingerprint identification.

1.9   Thesis Organization

Chapter 2 presents level 2 feature extraction technique from the fingerprint image. Image is enhanced by histogram equalization followed by Fourier transform. The enhanced gray scale image is converted into binary image. Segmentation is applied for extracting the Region of Interest (ROI) (area, which contain only useful information). Some post processing followed by minutiae extraction are carried out. Then matching algorithms are discussed for fingerprint.

Chapter 3 presents level 3 feature extraction technique. The state of art for work for dots, incipient ridges and pores extractions are explained. Then, the proposed approach for dots and incipient extraction are stated. Extraction consists of two steps: saddle point detection followed by tracing the valley. Saddle points are detected using power spectrum based filtering. Valleys are traced using Fast Marching Method

(FMM). Then some postprocessing methods are carried out for extracting dots and incipient.

Chapter 4 presents, fingerprint matching technique using level 2 and level 3 feature. Existing matching techniques are explained. Novel feature parameter sets for dots and incipient ridges are proposed using Delaunay triangulation. Then level 2 and level 3 feature based matching scores are fused using a novel score level fusion technique.

Chapter 5 presents, conclusion and describes the future work.

Chapter 2

Minutiae Based Feature Extraction

In the fingerprint feature hierarchy, minutiae are described as level 2 features. Extraction of minutiae rely heavily on quality of the fingerprint image and the fingerprint image is degraded due to abnormal formation of epidermal, occupational mark, and defective acquisition device. Some fingerprints do not contain well defined ridge structures, for which preprocessing is necessary to improve the quality. Then, the fingerprints are converted into a binary image for representing ridge and valley in the black and white representation. Segmentation is carried out to extract Region of Interest (ROI), which contains enough information of ridge and valley. Thinning operation is performed to bring the pixel width of ridge to a single pixel. Minutiae are detected using the concept of crossing number followed by some postprocessing technique, which is used for discarding false minutiae. All the preprocessing steps are discussed below in sequel.

2.1 Fingerprint Enhancement

Image enhancement is one of the important preprocessing step. Some additional error may be added due to the faulty sensor and different skin condition. In order to increase the contrast between ridge and valley, the broken ridges are connected and the spurious points are discarded using preprocessing. To enhance the image we utilize histogram equalization and Fourier Transform (FT). Histogram equalization stretches the pixel ranges so that the resultant image has a better contrast. Enhancement process is explained in the following steps.

1. The image is divided into 32×32 block, and represented as $f(x, y)$

2. Fourier Transform is applied to each block using

$$F(u, v) = \sum_{x=0}^{31} \sum_{y=0}^{31} f(x, y) \times exp\left\{-j2\pi \times (\frac{ux}{32} + \frac{vy}{32})\right\} \qquad (2.1)$$

   where u =0,1,...31 and v =0,1,...31.

3. Magnitude of the block is calculated from the FFT as $abs(F(u, v)) = |F(u, v)|$.

4. For enhancing contrast of a particular block by its dominant frequencies, the FFT of the block is multiplied by its magnitude

$$g(x, y) = F^{-1}\left\{F(u, v) \times |F(u, v)|^a\right\}$$
$$f(x, y) = \frac{1}{32 \times 32} \sum_{x=0}^{31} \sum_{y=0}^{31} F(u, v) \times exp\left\{j2\pi \times (\frac{ux}{32} + \frac{vy}{32})\right\} \qquad (2.2)$$

   where x =0,1,...31 and y =0,1,...31. Value of a is choosen as 0.5 (experimentally determined). Fourier Transform based enhancement is helpful for connecting some broken points on the ridges and also removes some spurious connection between ridges.

            (a)   (b)
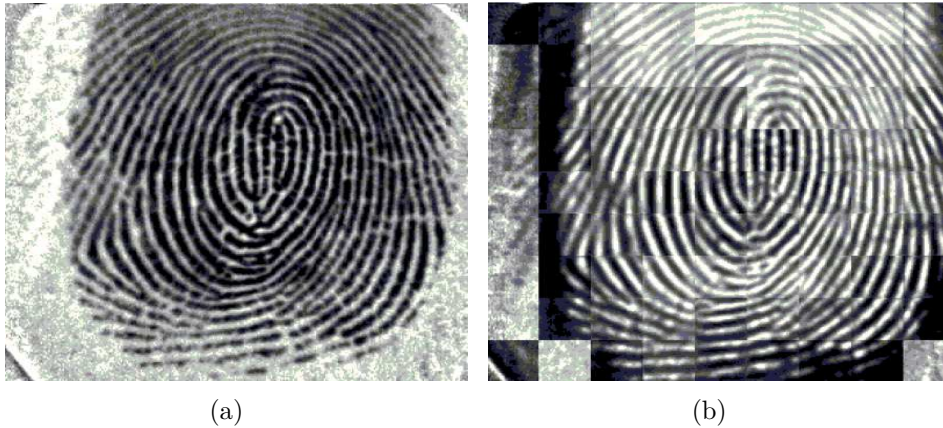
Figure 2.1: (a) Enhanced image using histogram equalization, (b) Enhanced image using Fourier transformation

2.2   Fingerprint Binarization

Binarization is used for converting an 8-bit gray scale image to a 1-bit black-and-white image. In a binarized fingerprint image, ridges are represented by pixels of value 0 (black) and valleys are represented by pixels of value 1 (white). A block adaptive binarization method is performed to obtain a binarized fingerprint as represented in Figure 2.2. The pixel is set to 1 if its value is larger than the mean intensity of the current block to which the pixel belongs to, else the pixel value is set to 0.

(a)   (b)
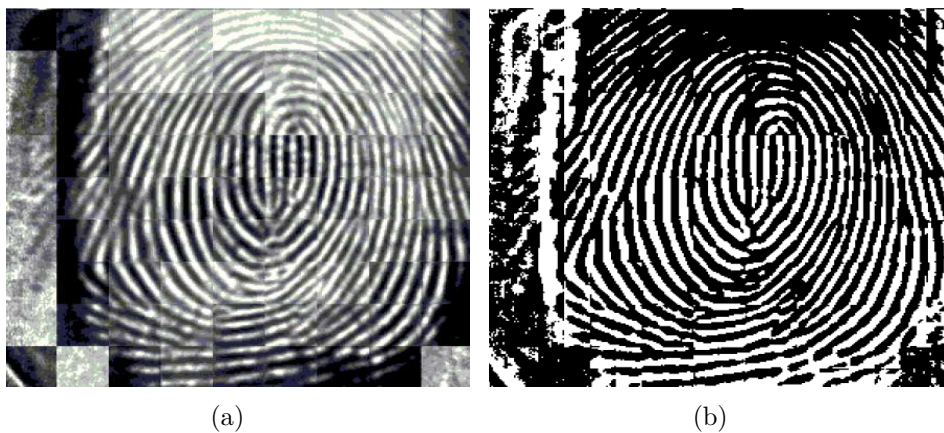
Figure 2.2: (a) Enhanced image, (b) Binary image

2.3   Image Segmentation

The segmentation is carried out for extracting only the ROI which contains relevant information. The block direction estimation followed by the morphological operation are employed for extracting ROI.

2.3.1   Block Direction Estimation

Block direction is estimated by the following algorithm.

1. The image is divided into non-overlapped block of size 16×16.

2. The gradient of the blocks along X-direction (g_x) and Y-direction (g_y) are calculated using Sobel filter.

3. Least square approximation of the block is calculated as:

$$\tan 2\alpha = 2 \sum \sum \frac{g_x \times g_y}{g_x^2 - g_y^2} \tag{2.3}$$

4. The certainty level of each block is calculated using the following equation.

$$E = \frac{\tan 2\alpha}{W \times W \times \sum \sum (g_x^2 + g_y^2)} \tag{2.4}$$

where W=16 is the size of the block. The block is considered if value of E is more than a calculated threshold, otherwise it is discarded.

2.3.2   Morphological Operation

Two morphological operation such as, "OPEN" and "CLOSE" are used for obtaining a ROI. "OPEN" is used to expand the image and remove the peaks introduced by background. However, "CLOSE" operation is used to shrink the image and eliminate small cavity. Boundary of the ROI are computed by subtracting closed area from opened area. The area inside the boundary are considered as ROI and rest are discarded. The detail description of operations are shown in Figure 2.3.

2.4   Feature Extraction

In order to extract the feature points (minutiae), thinning is performed on the ridges for which minutiae can be represented as a single pixel and distinguishable neighborhood pixels.

2.4.1   Thinning

Thinning operation is used to convert ridge of fingerprint into the 1-pixel width. An iterative parallel algorithm proposed by Mehtre [38] is applied. The image is scanned for several times, and a 3×3 window is used for the removal of redundant pixels.
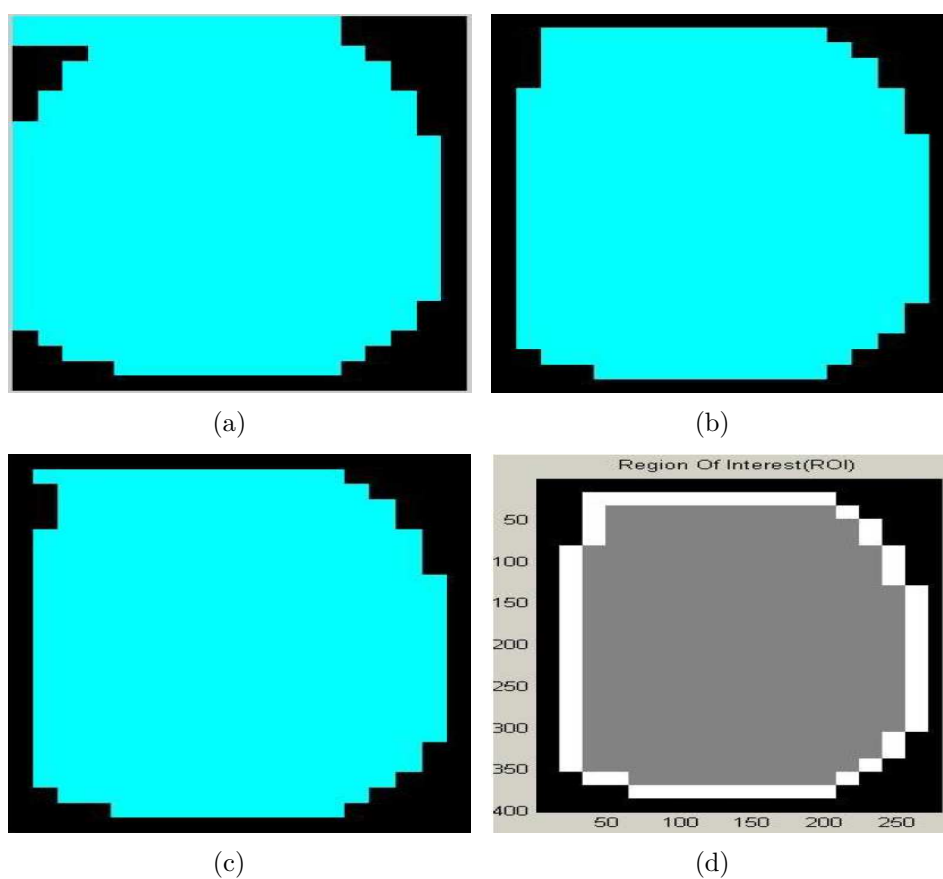
Figure 2.3: (a) ROI of original image, (b) ROI after applying open operation, (c) ROI after applying CLOSE operation, (d) ROI with boundary

2.4.2 Minutiae Extraction

Minutiae are extracted from the thinned fingerprint by *Crossing Number* (CN). A 3×3 window is taken from the fingerprint. Figure 2.4 (a) depicts the bifurcation, as the central pixel and three neighbor pixels have value 1. While Figure 2.4 (b) depicts the ridge ending where central pixel and one neighbor pixel has value 1.

2.5 Minutiae Postprocessing

Preprocessing stage is not able to discard all the false minutiae. Due to insufficient ink or more ink, some ridges break and some ridges have cross connection respectively. These spurious minutiae will affect the accuracy while matching. There might be false minutiae due to various reasons 2.5. As shown in Figure 2.5 (a) is a spike originating from ridge and piercing into the valley. A spike may connect two ridges to make a

0	1	0		0	0	0
0	1	0		0	1	0
1	0	1		0	0	1

(a)   (b)
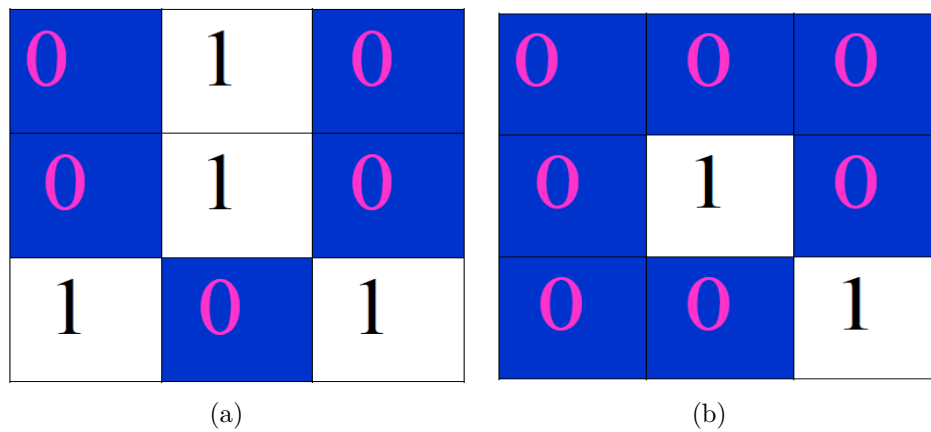
Figure 2.4: (a) Bifurcation, (b) Ridge ending

spurious minutiae as shown in Figure 2.5 (b). A third possible false minutia is due to two bifurcation are closely located as in Figure 2.5 (c). Fourth type is due to the broken ridge as in Figure 2.5 (d). Next type is similar to the fourth but one part of the broken ridge as in Figure 2.5 (e) is very small. Sixth type is also similar to fourth, but a small piece of the ridge is generated between two broken ridges as in Figure 2.5 (f). And the last false minutiae is due to a short ridge in Figure 2.5 (g). All the mentioned false minutiae are removed by using following techniques.
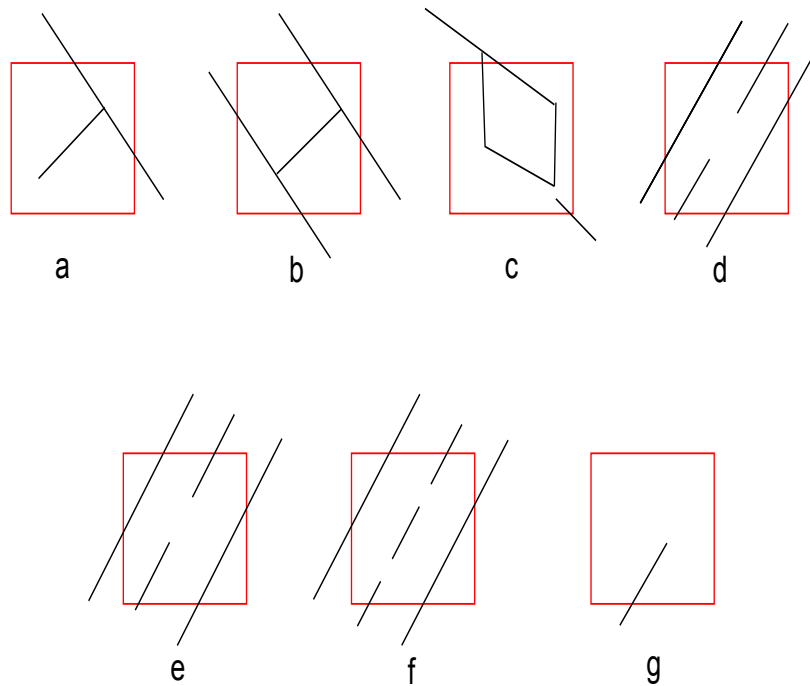
Figure 2.5: Spurious minutiae

1. let d be the average inter ridge width between two parallel neighboring ridges. If the distance between one ridge ending and one bifurcation is less than d then both the minutiae are removed.

2. If the distance between two bifurcation is less than d and belongs to same ridge then both the bifurcation are removed.

3. If the distance between two ridge ending is less than d and their orientation are almost in same direction then both the minutiae are discarded.

4. If the length of a ridge is less than d then both of its ridge ending are discarded.

2.6 Matching

Level 2 feature matching has been done is two steps: minutiae are aligned at a reference point and then matching is carried out. Approximate congruent triangle is used for calculating reference point and its parameter, which has been explained in Section 4.1. A translation and rotation invariant matching algorithm is applied, which involves following steps:

1. Intra-Fingerprint Minutiae Comparison table is constructed: one table for probe and another table for gallery.

2. Inter-Fingerprint Compatibility table is constructed.

3. Inter-Fingerprint Compatibility table is constructed by comparing probe and gallery intra-fingerprint compatibility table.

4. Inter-Fingerprint Compatibility table is traversed and tail entries are linked.

5. Compatible clusters are grouped and matching score is obtained.

2.7 Summary

In this chapter, minutiae based fingerprint identification has been described. Fingerprint quality is enhanced using histogram equalization and Fourier transform.

The adaptive thresholding method is used to binarize the enhanced image. In order to discard noisy region, the direction estimation and morphological operation has been applied. Ridges are thinned using an iterative parallel algorithm. Crossing number technique is applied for detecting minutiae. Some postprocessing technique has been used for eliminating spurious minutiae. For fingerprint matching, intra-fingerprint and inter-fingerprint compatibility table of BOZORTH3 of NBIS [39] has been followed.

Chapter 3

Level 3 Feature Extraction

Present Automatic Fingerprint Identification System (AFIS) schemes employ level 1 and level 2 features for matching. However, the level 2 features fail when complete fingerprint data are not available such as availability of a partial fingerprint. This limitation motivates the development of level 3 features such as dots, incipient ridges, ridge path deviation, width, shape, pores, edge contour, breaks, creases, and scars. The level 3 features are very minute, and demand a sensor with 1000 ppi resolution for acquisition. The standard resolution for AFIS is 500 ppi that is not sufficient for level 3 feature extraction. However, the advances of new fingerprint sensing technology with more than 1000 ppi resolution makes it possible to capture these features. The level 3 features are not included in current fingerprint feature standard. The Committee to Define an Extended Fingerprint Feature Set (CDEFFS) has decided to include these extended features in the Next Generation Identification (NGI) system of AFIS. National Institute of Standards and Technology (NIST) has conducted the first experiment on the extended feature set [40], where they have fused the level 3 features with minutiae key points. The performance increases with these extended features. However, the conducted experiment has few limitations. The level 3 features are selected manually by the expert. In addition, level 3 features includes more than one features that are to be used in the experiment that casts a question mark on which feature performs best as an individual entity.

Yi Chen *et al.* [35] proposed a technique for extracting dots and incipient, however this method consumes more time. In this chapter, a novel approach has been proposed to extract dots and incipient and ridges using tracing the valley. The

proposed approach has less computational complexity as compared to the reported method [35] which contains a high complexity skeletonization process. Pores is one of the prominent level 3 features and can be used in fingerprint identification [31,34]. In order to increase the accuracy, pores are taken along with dots and incipient ridges. Two related schemes have been studied in this chapter. A. K Jain *et al.* [31] has proposed a scheme using Gabor filter and wavelet transform. Manivanan N [34] has proposed pore extraction algorithm based on highpass filtering followed by correlation. We have employed the second scheme [34] due to its better performance on the noisy images. A matching process by considering all the extracted level 2 and level 3 features has been suggested and explained in Chapter 4.

3.1   Dots and Incipient Ridge Extraction

Dots and incipient ridges are two extended features, which are present on the valley of a fingerprint. Dots are short ridge units having size less than 0.02 inch, whereas incipient ridges are substantially thinner than normal ridges. From the state-of-art, it has been observed that their shape and size may be affected due to pressure difference. So, both features are considered as identical feature while matching.

3.1.1   Dots and Incipient Ridge Extraction using Phase Symmetry

Yi Chen *et al.* [35] proposed dots and incipient ridges extraction scheme which consists two stages: phase symmetry measurement and valley skeletonization. Dots and incipient ridges are having more phase symmetry than normal ridge, since they are very small as compared to the ridge.

Phase Symmetry

There are many ways of representing an image in terms of frequency. Here wavelet transform is used for analyzing the image. The advantage of wavelet transform is due to its local frequency information. This is achieved by using bank of filters where each filter is used to analyze a particular band of frequencies. A linear phase filter is

required for analyzing phase information. A wavelet based on complex valued Gabor filter is used, which consists of a pair of even and odd filter.

This can be achieved by convolving even and odd quadrature filter to the image. Let I be an image, A_n^e and A_n^o are even-symmetric and odd-symmetric wavelet at scale n. The response of the above filter is represented as,

$$[e_n(x,y), o_n(x,y)] = [I(x) * A_n^e, I(x,y) * A_n^o] \tag{3.1}$$

The response $e_n(x,y)$ and $o_n(x,y)$ are the real and imaginary part of complex valued frequency component. The amplitude of the wavelet transform is,

$$A_n(x,y) = \sqrt{e_n^2(x,y) + o_n^2(x,y)} \tag{3.2}$$

and the phase is given by,

$$\Phi_n(x,y) = arc\tan(e_n^2(x,y), o_n^2(x,y)) \tag{3.3}$$

At the point of symmetry, even-symmetric filter output is larger than odd-symmetric filter outputs. Filters with multiple scales are applied and a weighted average of the filter responses over multiple scales is formed. The symmetry value is defined as the normalized difference of the absolute value between outputs from even-symmetric and odd-symmetric filters as given by,

$$
\begin{aligned}
Sym(x,y) &= \frac{\sum\limits_n A_n(x,y)[|\cos(\Phi_n(x,y))| - |\sin(\Phi_n(x,y))|]}{\sum\limits_n A_n(x,y) + \varepsilon} \\
&= \frac{\sum\limits_n \lfloor [|e_n(x,y)| - |o_n(x,y)|] \rfloor}{\sum\limits_n A_n(x,y) + \varepsilon}
\end{aligned}
\tag{3.4}
$$

The ε is a small constant to prevent division by zero in the case where the signal is uniform and no filter response is obtained.

Skeletonization

Once local symmetry is estimated, the next step is to skeletonize the valley of the image. This is because dots and incipient ridges occur only on valleys between normal

friction ridges. Level set based continuous skeletonization is used for thickening (not one pixel thinning) proposed by Martin Rumpf *et al.* [41]. These methods detect the skeleton by looking for the valley of the Distance Transform (DT) of the image boundary. When distance transform is applied to an image, gray level intensities of points inside foreground regions are changed (intensity increases towards the center of the foreground) to show the distance to the closest boundary from each point. There are different sorts of the distance transform, depending upon which distance metric is being used to determine the distance between pixels. Here, chessboard distance has been employed. Then the local symmetric image is multiplied with skeletonized valley image to get an image which contains only dot and incipient ridge as shown in Figure 3.1 (d). Then center of dots and mid-point of the incipient ridge are found. Position and orientation of these points are taken as feature set.
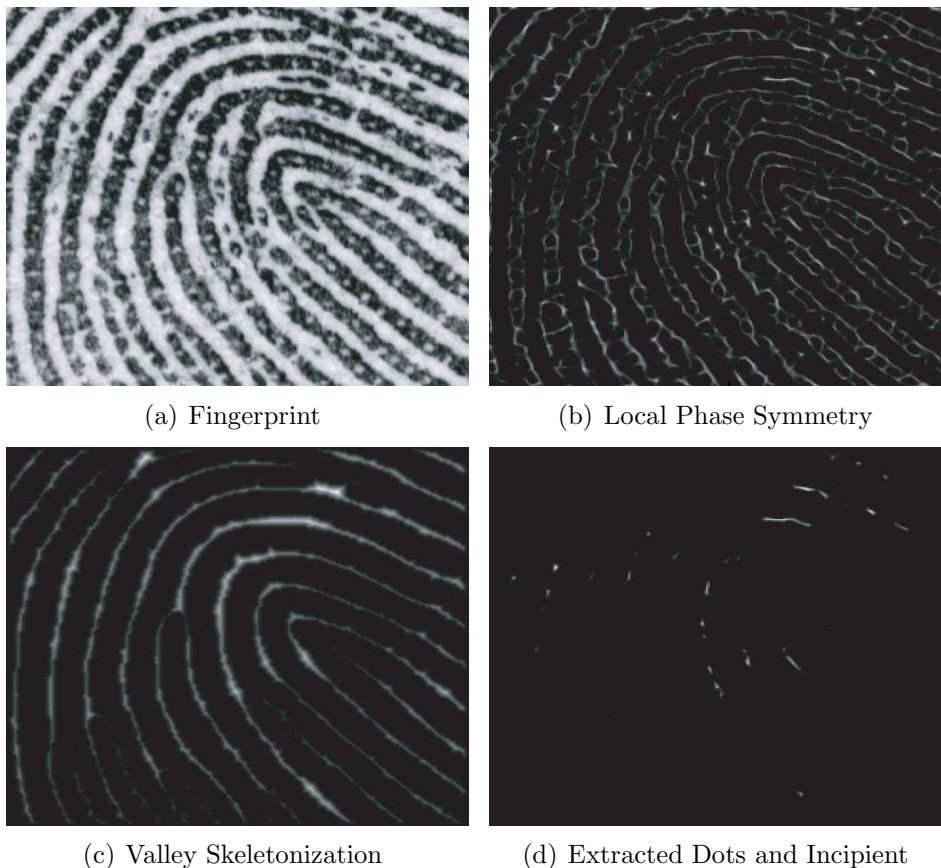

(a) Fingerprint   (b) Local Phase Symmetry

(c) Valley Skeletonization   (d) Extracted Dots and Incipient

Figure 3.1: Dots and incipient ridges extraction

3.1.2   Proposed Dots and Incipient Extraction by Tracing Valley

The extraction technique used in Section 3.1.1 involves thickening, which has computational complexity of $O(m \times n)$ [41], where m and n are number of pixels in rows and columns. Dots and incipient ridges are extracted by tracing valleys. Starting points have been found on the valley by analyzing the frequencies present in the fingerprint. Valleys are traced from the starting point using Fast Marching Method (FMM) [42]. Then an intensity checking method is used for finding these features. The proposed method has computational complexity $O(max(m, n) \times k)$, where k is the number of valleys present in the fingerprint.

Starting Point Extraction

Our primary objective is to select a set of points on valleys from which tracing of the valley can be started. Tracing is done in such a way that each traced point lies approximately on the middle of that valley. Better starting point provides a better tracing. Initially, a window is taken from the middle portion of the fingerprint. X-signature [43] of the window is calculated for analyzing the frequencies present in the window. X-signature is the representation of an image in terms of sinusoidal waves. The window consists of sinusoidal waves of different frequencies. Ridge valley pattern of a fingerprint image can be represented as a sinusoidal wave of constant frequency. In signal processing concept, if the speed of the signal is equal to the wavelength, then the frequency component contains only first harmonic. The frequency is calculated as,

$$Frequency = \frac{Speed}{Wavelength} = \frac{\lambda_r + \lambda_v}{\lambda} = 1 \tag{3.5}$$

where λ_r and λ_v is the width of the ridge and valley respectively. The above frequency represents the first harmonics.

To extract the ideal signal, all the frequencies above and below the first harmonics are suppressed. The lower frequency component is due to the presence of noise along with dots and incipient ridge on the valley, and the high-frequency component is

due to noise along with pores on the ridges. The ideal signal is obtained by the window based filtering [43] with its corresponding power spectrum. The processed X-signature is approximately close to a signal which contains only single frequency as shown in Figure 3.2(d). In single frequency representation of a fingerprint, ridges are represented as low peaks and valley are represented as high peaks. The top of high peak of the processed X-signature will be the center of the valley. As we need a starting point on each of the valleys on a fingerprint, window is taken from the middle of the image and vertically moved down. The reason for selecting the window in the middle of the image is to cover the maximum number of valleys with the minimum number of windows. The problem may arise near singular point and delta region. In order to get a starting point in these regions, we shift the window towards left and right horizontally until a starting point is identified.
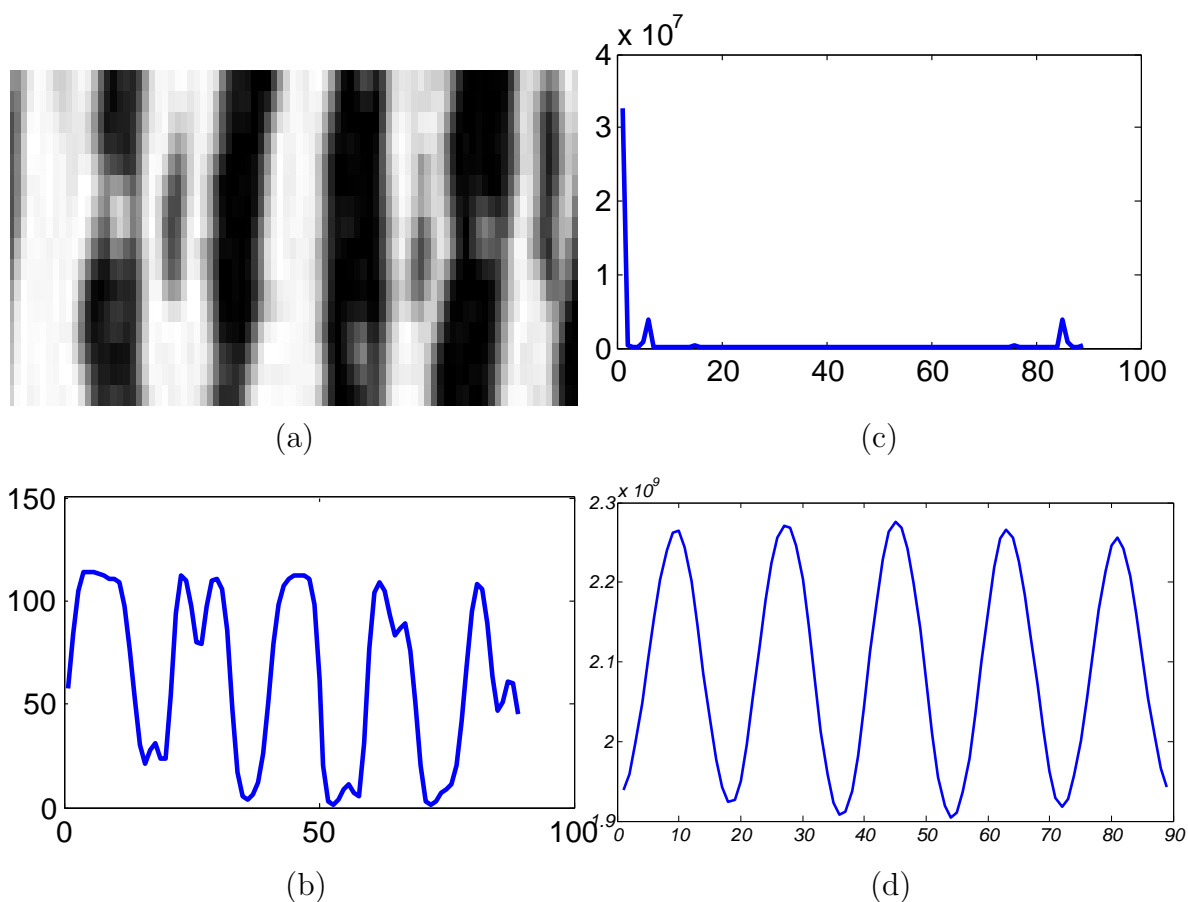

Figure 3.2: (a) Window from the middle part of fingerprint, (b) X-Signature of the window, (c) Power spectrum of the X-Signature, (d) Processed X-Signature

The X-signature and the corresponding power spectrum are shown in Figure 3.2. However, the point may be located either on white pixel area (valley) or on black pixel area (dots or incipient ridge). To know that, an intensity checking procedure is used. The intensity of the point is compared to a threshold computed experimentally. If the intensity is less than the threshold, it will be discarded as a starting point. If intensity is above the threshold, then entropy of the neighborhood of the point is calculated using

$$Entropy = -\sum_{i=0}^{i=255} P_j \log_2 P_j \tag{3.6}$$

where P_j is the probability that the difference between two adjacent pixel is i. Entropy based checking is done to know the presence of white noise on the dots and incipient ridges. If the starting point is on the white patch (noise) in the dots, then entropy of the neighborhood will be higher. So if entropy of the neighborhood is higher than a threshold value, then the point is discarded otherwise it is considered as a starting point. After finding the starting point, the next job is to trace the valley using Fast Marching Method (FMM). FMM [42] is utilized for image segmentation. In this thesis, we have used FMM for tracing valleys.

Fast Marching Method

The fast marching method is a numerical method for solving boundary value problems of the Eikonal equation. It is a special case of level set method for computing the propagation of front where the speed depends on the local position and is extremely fast scheme for solving the Eikonal equation. The following steps explain FMM and how it is used for tracing valley.

Interface Propagation

The interface is defined as the curve or surface, which separates inside and outside of a region. Interface propagation is defined as the motion of the interface in normal direction. Velocity of an interface is described by following steps:

1. A component depends on the local property of the interface.

2. A component belonging to global properties of the surface.

3. A component independent of the surface.

The Boundary Value Formulation

An interface which is strictly expanding or contracting is known as the boundary value formulation. A relation between arrival function and speed of the interface is established by the Eikonal equation and given as,

$$|\nabla T|\, F = 1 \tag{3.7}$$

where T is the arrival function and F is the speed of the interface. Arrival function has one more dimension than the surface. For example, if the surface is in R^2 then the arrival function will be in R^3. Interface is expanding when $F > 0$ and contracting when $F < 0$. FMM is the special case where the interface moves in one direction, whereas the initial value formulation does not impose this restriction.

Initial Value Formulation

In the initial value formulation, an interface may propagate back to points it has already propagated. It follows that the speed function F is no longer strictly greater or strictly less than 0 for all time. In order to facilitate this, a level set function is required.

Level Set Method and its Solution

Given an initial position for an interface τ, where τ is a closed curve in R^2. A speed function F, which gives the speed of τ in its normal direction. The level set method takes the perspective of viewing τ as the zero level set of a function $\Phi(x, t = 0)$ from R^3 to R. That is $\Phi(x, t = 0) = \pm d$, where d is a distance from x to τ, and the plus (minus) sign is chosen if the point x lies outside (inside) the initial surface τ. Using chain rule, an evolution equation for the interface can be written as,

$$\Phi_t + |\nabla \Phi|\, F = 0 \tag{3.8}$$

where Φ is the level set function, F is the speed function, and Φ_t represents the first derivative of Φ with respect to t. Solution to the above equation is given by,

$$\Phi_{ij}^{n+1} = \Phi_{ij}^n - \Delta t(\min{(D_{ij}^{+x}\phi, 0)}^2 \max(D_{ij}^{-y}\Phi, 0))^{1/2}$$
$$-\Delta t(\max{(D_{ij}^{-x}\Phi, 0)}^2 + \min{(D_{ij}^{+y}\Phi, 0)}^2)^{1/2}$$

(3.9)

where the speed $F = 1$ and the difference operator is defined as $D_{ij}^{+x}\Phi = (\Phi_{i+1,j} - \Phi_{i,j})/\Delta t$. This solution is for evolution of all the level sets corresponding to the front itself. So, this is a computationally expensive solution. An efficient technique called "narrow band approach" which works only in a neighborhood of the zero level set has been used for tracing. Using this concept, grid points are divided into alive, land mines or far away, depending on whether they are inside the band, near its boundary, or outside the band, respectively. One-cell version of this leads to fast marching method.

Fast Marching Level Set Method

If $F = F(x, y, z) > 0$ is a speed function, a monotonically advancing front whose level set equation is $\Phi_t + F(x, y, z)\,|\nabla T| = 0$ is given by,

$$T(x, t = 0) = \tau \tag{3.10}$$

In two-dimensional case, the interface is a propagating curve, zero level set is evolved along xy-plane. The $T(x, y)$ is the time at which the curve crosses the point (x, y). The surface will satisfy by Eikonal equation defined in equation 3.7.

According to equation 3.7, gradient of arrival time surface is inversely proportional to the speed of the front. Using approximation of the gradient, the solution of the equation (3.10) is given as,

$$\max{(D_{ij}^{-x}T, 0)}^2 + \min{(D_{ij}^{+x}T, 0)}^2 + \max{(D_{ij}^{-y}T, 0)}^2 +$$
$$\min{(D_{ij}^{+y}T, 0)}^2] = \frac{1}{F^2}$$

(3.11)

where $T(x, 0) = 0$.

Rouy and Tourin has found a less diffusive iterative algorithm for computing the solution for Eikonal equation which is given as,

$$\max\left(\max(D_{ij}^{-x}T, 0), -\min(D_{ij}^{+x}T, 0)\right)^2 +$$

$$\max\left(\max(D_{ij}^{-y}T, 0), -\min(D_{ij}^{-y}T, 0))^2\right] = \frac{1}{F_{ij}} \tag{3.12}$$

The important aspect of constructing Fast Marching Level Set Method algorithm is to estimate propagation of front in an upwind manner with speed F_{ij} and its direction is normal at each grid point. Here the set of grid points $j = 1$ corresponds to y axis, and we assume that $F_{ij} > 0$. So, the algorithm solves the above equation by increasing the value of T from its smallest value. The Front of the surface sweeps in upwind direction with set of points in the band around it. New points are formed in narrow-band structure by discarding the existing surface points. Next, a grid point is selected and updated within the current narrow-band using the following algorithm.

1. Intialize

   (a) (Alive points: shaded points): Let A be the set of all grid points $i, j = 1$; set $T_{i,1} = 0.0$ for all points in A.

   (b) (Narrow-band points: circles): Let narrow-band be the set of all grid points $i, j = 2$; set $T_{i,1} = \frac{dy}{F_{ij}}$ for all points in narrow-band.

   (c) (Far away points: rectangles): Let far away be the set of all grid points $i, j > 2$; set $T_{i,j} = \infty$ for all points in far away.

2. Marching Forward

   (a) Begin Loop: Let $(i_{\min}, j_{\min})$ be the point in narrow-band with the smallest value for T.

   (b) Add the point $(i_{\min}, j_{\min})$ to A; remove it from narrow-band.

   (c) Tag as neighbors any points $(i_{\min} - 1, j_{\min}), (i_{\min} + 1, j_{\min}), (i_{\min}, j_{\min} - 1), (i_{\min}, j_{\min}+1)$ that are either in narrow-band or far away. If the neighbor is far away, remove it from that list and add it to the set narrow-band.

   (d) Recompute the values of T at all neighbors according to equation 3.12, selecting the largest possible solution to the quadratic equation.

(e) Return to loop.

The important aspect of constructing Fast Marching Level Set Method algorithm is to estimate propagation of front in upwind direction with a speed of F_{ij} and its direction is normal at each grid point.

Feature Extraction

In this scheme, we have used FMM for tracing valleys of the fingerprint. Instead of taking initial point (alive point as defined in FMM) along y-axis as FMM, the set of points are taken as explained in Section 3.1.2. We are able to propagate towards right and left of the saddle point which is normal to the interface in anti-clockwise and clockwise direction respectively. While tracing, a window is taken around the traced point. If $I(i, j) < \alpha$, where (i, j) is any pixel in the window, and α is a gray level intensity value, then a connected component is constructed by considering the range of the intensity value 0 to α. These connected components include dots, incipient ridges and noise. The CDEFFS standardizes that the sizes of dots and incipient ridges are less than 0.02 inch. So all the extracted components with size more than 0.02 inch (part of a ridge) are discarded. Next, centroids as well as directions of remaining extracted components are computed. The fingerprint with traced valley, and the extracted dots and incipient ridge are shown in Figures 3.3 (a) and 3.3 (b) respectively.
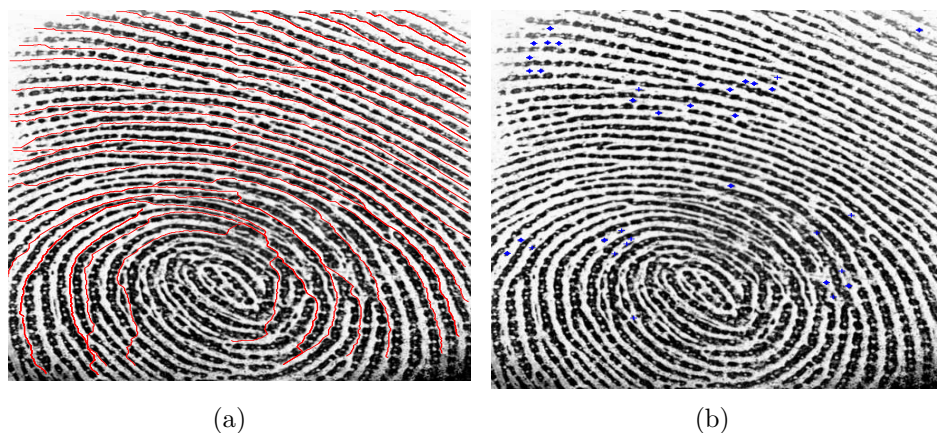

(a)   (b)

Figure 3.3: (a) Traced image, (b) Dots and incipient ridges are shown in '*' and '+' respectively

3.2   Pore Extraction

3.2.1   Gabor and Wavelet Transform Based Pore Extraction

A. K Jain *et al.* [31] proposed pores extraction method using the Gabor filter and Wavelet transform. The Gabor filter [20] is used for enhancing fingerprint image. The filter is given as,

$$G(x, y : \theta, f) = exp\left\{-\frac{1}{2}\left[\frac{x_\Theta^2}{\sigma_x^2} + \frac{y_\theta^2}{\sigma_y^2}\right] Cos(2\pi f x_\theta)\right\} \qquad (3.13)$$

where θ, f, σ_x and σ_y are orientation, frequency, standard deviation along X-axis and Y-axis respectively and can be determined from ridge frequency and orientation of fingerprint. The point (x_θ, y_θ) is a clockwise rotation of $(90 - \theta)$ of the point (x, y). The ridge can be well separated from the valley by using the Gabor filter. By using this filter, pores are filled (which are considered as noise on macro level) and only the ridges are highlighted. Then the original image is added to the filtered image. In the resulting image, contrast between the pores and ridge is low. For extracting pores, a band pass filter is used to capture a high negative frequency response as intensity varies suddenly in pores. Wavelet transform [44] is used due to its localization property. The wavelet transform of the fingerprint image $f(x, y) \in R^2$ with the frequency response W is given as,

$$W(s, a, b) = \frac{1}{\sqrt{s}} \int\int_{R^2} f(x, y)\Phi(\frac{x - a}{s}, \frac{y - b}{s})dxdy \qquad (3.14)$$

where s is the scale factor and, a and b are the shifting parameters. Scale factor makes the wavelet transform as a bandpass filter. The filter response is normalized using min-max normalization. Pores are represented as small blob with low intensity. By adding both Gabor and wavelet filter response, more enhanced fingerprint with prominent pores are obtained. Then a threshold is applied to extract pores having blob of size less than 40 pixels. The corresponding steps are shown in Figure 3.4. The pore extraction algorithm is more efficient than skeletonization based algorithm, which are sensitive to noise.
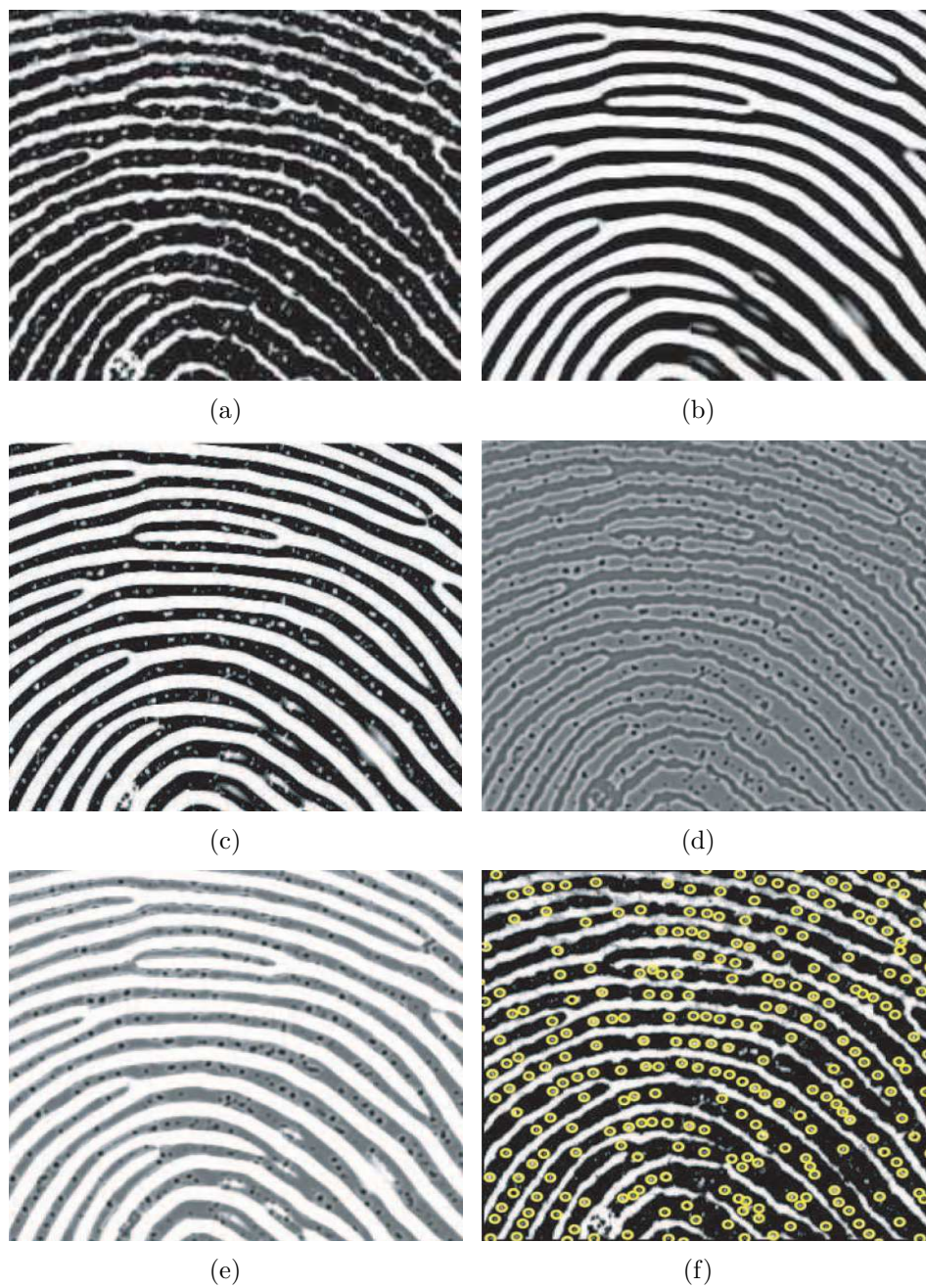
Figure 3.4: Pores extraction: **(a)** Fingerprint image, **(b)** Enhancement of image (a) using Gabor Filter, **(c)** Linear combination of (a) and (b), **(d)** Wavelet response of image (a), **(e)** Linear combination of (b) and (d), **(f)** Extracted pores

3.2.2   Filter and Correlation Based Pore Extraction

N. Manivanan [34] has proposed a pore extraction method based on highpass filtering followed by correlation. According to the image processing concept, a space domain image can be converted into Fourier domain that represents a frequency spectrum of

different bands. Each image structure can be analyzed by using specific frequency range. Edges in an image contain a high frequency component. With more number of transitions within an image, a high frequency is obtained. As pores are white circle on the ridge, it contains high frequency and a highpass filter is used to extract the pores. A correlation is used to find the similarity between two images. The correlation of two signal $g(x, y)$ and $h(x, y)$ is given as,

$$C(X, Y) = \int \int g(\varepsilon, \eta) h(\varepsilon - X, \eta - Y) \tag{3.15}$$

where ε and η are dummy variables used for evaluating integration. A 64×64 block from an image is taken. Fourier transform and a highpass filter with cutoff frequency 15 in both X and Y direction are applied for extracting pores. Then, the resulting image is correlated with a binary circle having radius of three pixels. The equation of the circle is given as,

$$r(x, y) = \begin{cases} 1, x^2 + y^2 \leq 3 \\ 0, Otherwise \end{cases} \tag{3.16}$$

Then this image is transfered to Fourier domain and its complex conjugate is computed as,

$$\begin{aligned} \text{R(X, Y)} &= \text{FT}[\text{r(x, y)}] \\ H(X, Y) &= R^*(X, Y) \end{aligned} \tag{3.17}$$

where $R(X, Y)$ is the complex conjugate of $r(x, y)$ in Fourier domain.

3.3   Summary

In this chapter, a level 3 feature extraction technique has been described. Dots and incipient ridges have been extracted using phase symmetry and skeletonization method. A proposed valley tracing scheme based on dots and incipient ridges have been explained. The proposed extraction technique has less computational complexity than the earlier method. Also, the extraction of pores have been described in this chapter. In one approach, Gabor and wavelet transform is applied for the extraction
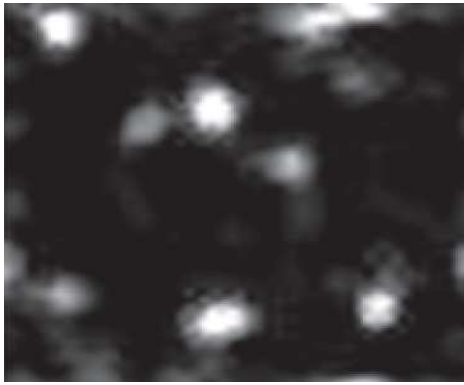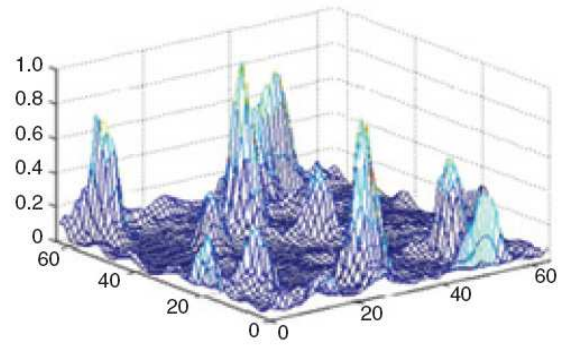
Figure 3.5: (a) Image containing pores. (b) 3D mesh representation of pores

of pores. In another approach, pores are detected using highpass filter followed by correlation method.

Chapter 4

Level 3 Feature based Matching

A typical fingerprint matching algorithm finds a degree of similarity between two images. This degree of similarity can be measured either by a decision (one for accept and zero for reject) or by a score (between zero to one). Most of the matching technique compares different features. However, some of the matching algorithms use the fingerprint image directly. The matching algorithms suggested in the literature are suitable for full fingerprint image. Hence, there lies a challenge in partial fingerprint matching. Fingerprint matching can be divided among three categories namely: correlation based matching, minutiae based matching, and ridge feature based matching. In this thesis, we have used ridge feature based matching along with minutiae. Three conventional matching techniques are explained as follows.

- **Correlation based matching:** Correlation between two fingerprints are found for different alignment. Let I and T are input and template fingerprint image respectively. Sum of Difference (SSD) is a measure of similarity between two images. For same image SSD is zero. More the difference between two images, more the SSD value. SSD is evaluated as,

$$SSD(T, I) = \|T - I\| = (T - I)^T(T - I) = \|T\|^2 + \|I\|^2 - 2T^T I \qquad (4.1)$$

  $T^T I$ is the correlation between images T and I. As $\|T\|^2$ and $\|I\|^2$ are constant, SSD depends upon correlation ($2T^T I$). Smaller the correlation value, more the similarity. An intrinsic problem occurs while taking a translated and rotated fingerprint image. Let's consider $I^{(\Delta x, \Delta y, \theta)}$ be the displaced and rotated input

image with respect to template image T. The correlation between the input and template image can be defined as,

$$CC(T, I^{(\Delta x, \Delta y, \theta)}) = T^T I^{(\Delta x, \Delta y, \theta)} \tag{4.2}$$

In order to increase the matching score, correlation is maximized and the matching score is defined as,

$$M(T, I) = \max_{\Delta x, \Delta y, \theta} CC(T, I^{(\Delta x, \Delta y, \theta)}) \tag{4.3}$$

In practice, correlation based matching is not suitable due to non-linear distortion, skin condition, fingerprint pressure difference and also it is computationally expensive.

- **Minutiae based matching:** Minutiae based matching is the most popular fingerprint matching approach. In this technique, a fingerprint is represented by a feature vector which contains minutiae. Each minutia can be described by location, orientation and type of minutiae. However, most of the current matching algorithms use location and orientation of a minutia and can be represented as $m = x, y, \theta$, where θ is orientation, x and y are X-coordinate and Y-coordinate respectively. Let T and I represent the set of minutiae for template and input image expressed as,

$$
\begin{aligned}
T &= \{m_1, m_2, m_3, ..., m_m\}, m_i = \{x_i, y_i, \theta_i\}, i = 1..m \\
I &= \{m'_1, m'_2, m'_3, ..., m'_m\}, m'_j = \{x'_j, y_j, \theta'_j\}, j = 1..n
\end{aligned} \tag{4.4}
$$

m and n are number of minutiae in template and input fingerprint.

Registration is carried out in order to align input image with template image. Let $align()$ be a function that maps a minutia m_i from I (input image) to m'_i from T (template image). Let $[\Delta x, \Delta y, \theta]$ be the displacement and counter clockwise rotation of I with respect to T. Then $align()$ is defined as,

$$align(m_i = \{x_i, y_i, \theta_i\}) = m'_i = \{x'_i, y'_i, \theta'_i\} \tag{4.5}$$

$$\begin{bmatrix} x'_i \\ y'_i \end{bmatrix} = \begin{bmatrix} \cos\theta & -\sin\theta \\ \sin\theta & \cos\theta \end{bmatrix} \begin{bmatrix} x_i \\ y_i \end{bmatrix} + \begin{bmatrix} \Delta x \\ \Delta y \end{bmatrix} \tag{4.6}$$

$$mm(m'_j, m_i) = \begin{cases} 1, sd(m'_j, m_i) \leq r, dd(m'_j, m_i) \leq \theta \\ 0, otherwise \end{cases} \tag{4.7}$$

where $mm()$ is a function that returns 1 when there is a match between m'_j and m_i. There will be a match between m'_i and m_j if Euclidean distance of position and orientation is less than their respective thresholds. The Euclidean distance for position and orientation is given as,

$$sd(m'_j, m_i) = \sqrt{(x'_j - x_i)^2 + (y'_j - y'_i)^2} \leq r \tag{4.8}$$

$$dd(m'_j, m_i) = min(|\theta'_j - \theta_i|, 360 - |\theta'_j - \theta_i|) \leq \theta \tag{4.9}$$

where, r and θ are the threshold for position and orientation respectively.

The matching problem can be formulated as,

$$\underset{\Delta x, \Delta y, \theta, p}{maximize} \sum_{i=1}^{m} mm(map_{\Delta x, \Delta y, \theta}(m'_{p(i)}), m_i) \tag{4.10}$$

where $p(i)$ is a function which determines the correspondence between input and template minutiae.

- **Ridge feature based matching:** There are many reasons for considering more features besides minutiae. It is very difficult for extracting minutiae from poor-quality fingerprint image. Minutiae based matching techniques fail to match when the fingerprint contains less than 40 numbers of minutiae. In order to avoid these cases, more minute features are used. By considering additional features along with minutiae will increase the robustness and accuracy.

In this thesis, pores, dots, and incipient ridges are used as feature for fingerprint matching. To increase the matching accuracy, different fusion techniques are used. The fusion can be done at various levels such as feature level, match score level, and at decision level. In feature level fusion, multiple features are given to the matching algorithm, and one matching score is obtained. In match score level fusion, each feature is matched independently, and a score is obtained. Then the total matching scores are fused using score fusion technique like *sum rule* and *kernel method*. Decision level fusion is the improved version of match score fusion in which match scores are fused based on some decision fusion rule. In the proposed work, level 2 and level 3 feature has been fused using score level fusion. Delaunay triangulation is used for matching. Pores are also considered for matching. Pores are extracted using the technique as explained in Section 3.2.2. A pore based matching also has been done using a robust affine iterative closest point algorithm. Block diagram for the fusion technique has been shown in Figure 4.1.
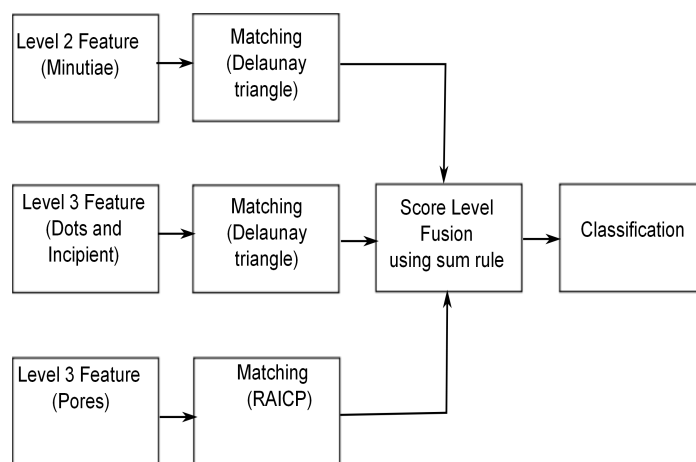

Figure 4.1: Block diagram of score level fusion

4.1   Proposed Dots and Incipient Based Matching using Delaunay Triangulation

Level 2 and level 3 features are extracted using the method as described in Chapter 2 and Chapter 3 respectively. Before matching, the input minutiae set P (all features

including level 2 and level 3 features) should be calibrated according to template minutiae set T within the same coordinate system by calculating translation, rotation, and deformation of input fingerprint with respect to template fingerprint. A reference point is needed to calculate these variables. One of the easiest methods for a reference point is a singular point. But in case of full to partial matching, input fingerprint hardly contains singular point. Skea [45] proposed an approximate congruent triangle which describes the minutiae spatial relation and degree of fingerprint deformation and can be used as reference point. $P' \subset P$ and $T' \subset T$ are the sets of points containing only level 2 features of input and template fingerprint respectively. For calculating reference point, similar vector triangle is used [45, 46]. Delaunay triangle is constructed by using extracted level 2 feature points. For calculating calibration parameter, a pair of matching triangles are found. We have compared triangle pair until we get a matching pair. Calibration parameters are calculated from the matched triangle pair. Edge and angle deformation of matched triangle pair are used for calculating those parameters. Edge and angle deformation is calculated as,

Edge deformation:

$$E1 = eA1/eB1$$
$$E2 = eA2/eB2 \tag{4.11}$$
$$E3 = eA3/eB3$$

Rotation deformation:

$$A1 = (A\alpha1 - A\beta1) - (A\alpha2 - A\beta2)$$
$$A2 = (A\beta1 - A\gamma1) - (A\beta2 - A\gamma2) \tag{4.12}$$
$$A3 = (A\gamma1 - A\alpha1) - (A\gamma2 - A\alpha2)$$

where, $eA1$, $eA2$ and, $eA3$ are edges of the triangle from input minutiae set. $eB1$, $eB2$, $eB3$ are edges of the triangle from template minutiae set. Similarly, $A\alpha1$, $A\beta1$ and, $A\gamma1$ are angles of the triangle from input minutiae set. $A\alpha2$, $A\beta2$ and, $A\gamma2$ are angles of the triangle from template minutiae set.

If the difference of above calculated parameter are within the calculated threshold then the two triangles are said to be similar, which can be mathematically represented as,

$$|E1 - E2| < th1$$
$$|E2 - E3| < th2 \tag{4.13}$$
$$|E3 - E1| < th3$$

$$|A1 - A2| < th4$$
$$|A2 - A3| < th5 \tag{4.14}$$
$$|A3 - A1| < th6$$

After positioning reference point, translation, rotation, and deformation has been calculated of the fingerprint in order to calibrate both fingerprints in the same coordinate system.

Deformation Parameter:

$$\text{scale\_rate} = \frac{E1 + E2 + E3}{3.0} \tag{4.15}$$

Directional rotation parameter:

$$\text{rotate\_rate} = \frac{A1 + A2 + A3}{3.0} \tag{4.16}$$

Now we have converted the input feature set P into the same coordinate system as template T by using Hough Conversion formula and above parameter.

$$\begin{pmatrix} X' \\ Y' \end{pmatrix} = \begin{pmatrix} scale\_rate * \cos(rotate\_scale) & -scale\_rate * \sin(rotate\_scale) \\ scale\_rate * \sin(rotate\_scale) & scale\_rate * \cos(rotate\_scale) \end{pmatrix}$$
$$\times \begin{pmatrix} dx \\ dy \end{pmatrix} + \begin{pmatrix} X \\ Y \end{pmatrix} \tag{4.17}$$

where, $\begin{pmatrix} dx \\ dy \end{pmatrix}$ is translation parameter is set to zero. (X, Y) and (X', Y') are point in input image before and after calibration respectively.

Level 2 and level 3 features have been used for full-to-partial matching. Due to uniqueness, local stability, structural stability, and linear time complexity, Delaunay triangulation [46, 47] gives very good performance in matching. Delaunay triangulation has already been used with level-2 features for fingerprint indexing and identification. However, we have used Delaunay triangulation not only for matching but also for establishing relation between level 2 and level 3 features. From minutiae set, Delaunay triangle is formed using following steps.

- Given n minutiae points, a Voronoi diagram is constructed in such a way that each region of the diagram will contain one minutiae.

- Delaunay triangulation is constructed by joining the minutiae in the neighborhood Voronoi regions.

Delaunay triangle is constructed by using minutiae set. Delaunay triangulation, which is constructed from the input image is compared with the stored triangulation (gallery) by using a set of feature. In a conventional Delaunay triangle matching, if input has K triangles and template has L triangles, then total number of comparison is $K \times L$ as one triangle in template Delaunay triangle is compared to L triangles in gallery Delaunay triangle. In addition to that, there is a chance that may not satisfy structural stability. We have proposed an efficient method which takes $K + L$ comparison and also maintains structural stability. For template Delaunay triangle, three sides of each triangle are sorted continuously in an array A. All the triplets are placed in such a way that $A[i] > A[i + 1] > A[i + 2]$, $A[i] > A[i + 3]$, $i = 1$ to M, $i\%3 = 1$, $(i + 1)\%3 = 2$, $(i + 2)\%3 = 0$, $M = 3 \times K$, where A is an array which contains the sides of triangle, M is size of array and K is the number of triangles. Similar procedure has been followed for storing template information in array T which contains N number of minutiae where $N = 3 \times L$ and $N > M$. Triangle edge triplets are stored as special pattern of sorted order so that a special case of merge sort can be employed. This sorting technique takes $O(K + L)$ time complexity for sorting two sorted array of size K and L. This sorting technique is used for a preliminary matching as described in Algorithm 1. In this algorithm, all compatible pairs from A

and T are figured out and considered for matching. Mahalanobis distances for edge and angle of the triangle pair are calculated. Edge triplets of a compatible pair are stored in X and Y, angles are stored in α and β. Then the Mahalanobis distance can be calculated as,

$$d(X,Y) = \sqrt{(X - Y)S^{-1}(X - Y)^T}$$
$$\phi(\alpha, \beta) = \sqrt{(\alpha - \beta)\theta^{-1}(\alpha - \beta)^T}$$

(4.18)

where S^{-1} and θ^{-1} are covariance matrix, $(X - Y)^T$ and $(\alpha - \beta)^T$ are transpose matrix for edge and angle respectively. Triangle pair is considered as a matching pair if $d(X,Y)$ and $\phi(\alpha, \beta)$ are less than the calculated threshold values. This process is carried out for all triangle pairs. A score of six is added for a matching triangle pair as it consists of there edges and three angles.

For matching using level 3 feature, spatial relation has been established with the neighboring minutiae. As dots and incipient ridges are present on the valley, it will lie either inside the triangle or on the edge of the Delaunay triangle which is already constructed using minutiae. We have compared only those triangles which contain level 3 features. If k and l are the number of dots and incipient ridges of input and template image respectively then total number of comparison is $k \times l$, where $k \times l < M \times N$. Let $\{l_{i1}, l_{i2}, l_{i3}\}$ and $\{\alpha_1, \alpha_2, \alpha_3\}$ are the edges and angle of a triangle from input image where, $l_{i1} > l_{i2} > l_{i3}$ and l_{ij} is non-adjacent to α_j, $j = 1, 2, 3$. When a dot is present inside the triangle then a new set of feature vector is extracted by connecting the dots to each corner of the triangle. These features are length of line connecting a dot to each corner and two angles sustained at each corner. When Il_1 is connecting to dot and α_1, α_{12} and α_{13} are sustained at α_1 as shown in Figure 4.2. When a dot is on the edge of the triangle then length of the line connecting to dot, and corner of the triangle is considered as a feature vector. Similar convention has been adopted for gallery set where edge and angle are defined as $\{l_{t1}, l_{t2}, l_{t3}\}$ and $\{\beta_1, \beta_2, \beta_3\}$ respectively. There is a match of an input triangle with gallery triangle if the following conditions are satisfied,

$$\mathrm{l}_{ij} - \mathrm{l}_{tj} < Th\_length$$
$$\alpha_j - \beta_j < Th\_angle1$$
$$Il_j - Tl_j < Th\_length\_dot \tag{4.19}$$
$$(\alpha_{xy1} - \beta_{xy1}) - (\alpha_{xy2} - \beta_{xy2}) < Th\_angle\_dot$$

where j=1, 2, 3 and $x = 1, 2, 3$, $x \neq y1 \neq y2$. Th_length, Th_angle1, Th_length_dot and Th_angle_dot are calculated threshold values. The above conditions are applicable if level 3 features are inside the triangle. If it is on the edge of the triangle, then third equation of 4.19 is modified as $Iml_{1o} - Tml_{1o} - (Iml_{2o} - Tml_{2o}) < th\_midlength$ and last equation is dropped. For a matching pair of triangles which contains level 3 features, a score of fifteen is added. *Sum rule* has been adopted for fusing level 2 and level 3 match score.

Algorithm 1 Triangle Pair Selection

Require: $A[1 : M], T[1 : N]$
Ensure: $Matched\_Array\_Index[1 : 2 \times K]$ contains all the matching pair index of A and T
1: Initialize: $Matched\_Array\_Index[1 : 2 \times K] = 0$, $j = 1$,$p = 1$, $K = M/3$
2: **for** $k = 1$ to K **do**
3:    **if** $A[i] \simeq T[j] \cap A[i + 1] \simeq T[j + 1] \cap A[i + 2] \simeq T[j + 2]$ **then**
4:       $Matched\_Array\_Index[p] = i$
5:       $Matched\_Array\_Index[p + 1] = j$
6:       $p = p + 2$
7:       $i = i + 3$
8:       $j = j + 3$
9:    **else if** $A[i] > T[j]$ **then**
10:       $i = i + 3$
11:    **else**
12:       $j = j + 3$
13:    **end if**
14: **end for**

4.2 Matching of Pores using RAICP Algorithm with Bidirectional Distance

Iterative Closest Point (ICP) algorithm [48] is one of the best techniques for point set registration problem. ICP algorithm iteratively aligns two sets of point and computes
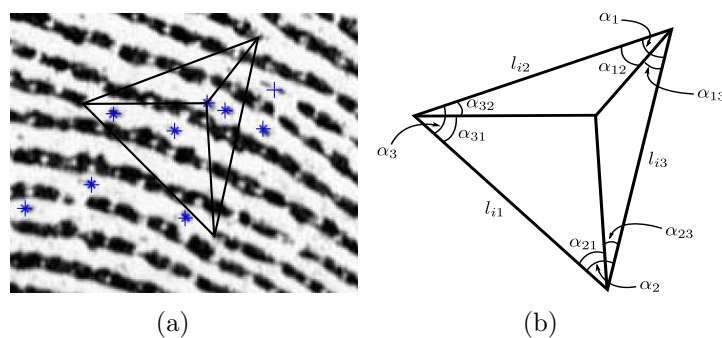
Figure 4.2: (a) Delaunay triangle constructed using minutiae, (b) Features extracted from triangle

translation and rotation vector by minimizing square distance. These transformation vectors are used to reconstruct one set of point with respect to other sets of point. This algorithm is working fine for rigid registration, but do not work for non-rigid registration. Fingerprint image shows non-rigid property due to the pressure variation while a fingerprint is taken either explicitly or implicitly. A registration technique is needed for fingerprint, which will tackle non-rigid behavior. Zhu. J *etal.* [49] proposed an algorithm which handles the non-rigid behavior by using affine transformation. Affine transformation is an ill-posed problem as the transformation vector may be zero. This is converted into a well-posed problem by calculating bidirectional distance for the least square formulation and is solved by the original ICP algorithm. This bidirectional distance also monotonically converges to a local minimum. Further, to obtain the best matching between two sets of points, Independent Component Analysis (ICA) is used for evaluating the initial parameter.

ICP Algorithm

Lets consider two sets of point, data shape P (input data) $P = \{p_i\}_{i=1}^{N_p}(N_p \in N)$ and a model shape $Q = \{q_j\}_{j=1}^{N_q}(N_q \in N)$ (gallery data). T is a transformation vector used to align P with respect to Q. Hence the least square distance between P and Q can be calculated as,

$$\min_{T, j \in \{1,2,...,N_q\}} \left(\sum_{i=1}^{N_p} \|T(p_i) - q_j\|^2 \right) \tag{4.20}$$

According to traditional ICP algorithm, T is a rigid transformation (translational

and rotational transformation). Now by using these parameters, least square distance function is represented as,

$$\min_{T, j \in \{1,2,\ldots,N_q\}} \left(\sum_{i=1}^{N_p} \|Rp_i + t - q_j\|^2 \right) \tag{4.21}$$

$$such\, that,\, R^T R = I_m, \det(R) = 1$$

where $R \in R^{m \times m}$ is a rotation matrix and $t \in R^m$ is a translation vector. According to ICP algorithm, the least square distance function is solved by two iterative steps. A new correspondence is calculated by $(k-1)^{th}$ transformation (R_{k-1}, t_{k-1}) as,

$$c_k(i) = \arg\min_{j \in \{1,2,\ldots,N_p\}} \|R_{k-1}p_i + t_{k-1} - q_j\|^2 \tag{4.22}$$

Now, th rigid transformation (R_k, t_k) is computed using current correspondence $\{i, C_k(i)\}_{i=1}^{N_p}$ as,

$$(R_k, t_k) = \arg\min_{R^T R = I_m, \det(R)=1, t} \left(\sum_{i=1}^{N_p} \|Rp_i + t - q_{c_k(i)}\|^2 \right) \tag{4.23}$$

Affine Transformation

The transformation function is modified by using affine transformation instead of rigid transformation. A bidirectional least square distance function is used to make the transformation as well-posed. The modified ICP algorithm is called as robust affine ICP algorithm. Affine transformation includes two parameters, that is affine matrix and translation vector which can be represented as,

$$x' = Ax + t \tag{4.24}$$

where the affine matrix A is an invertible matrix and t is a translation vector. Now the least square distance function can be modified by using affine transformation as,

$$\min_{A,t,j\in\{1,2,...,N_q\}} \left(\sum_{i=1}^{N_p} \|Rp_i + t - q_j\|^2 \right) \tag{4.25}$$

$$such that \det(a) \neq 0$$

Robust affine ICP algorithm

In 4.25, when $det(A)$ converges to zero, the registration becomes an ill-posed problem, hence all the data points of P will transform to few data points on Q. This ill-posed registration is transformed to well-posed by using bidirectional distance in the least square distance function. Then the least square distance function with bidirectional distance is defined as,

$$\min_{\substack{A,t,j\in\{1,2,...,N_p\} \\ j\in\{1,2,...,N_q\}}} \left(\sum_{i=1}^{N_p} \|Ap_i + t - q_j\|^2 + \sum_{j=1}^{N_q} \|Rp_i + t - q_j\|^2 \right) \tag{4.26}$$

In equation 4.26, the distance function consists of sum of two terms. $\sum_{i=1}^{N_p} \|Ap_i + t - q_j\|^2$ is used to transform P to register with Q is called as forward square distance and $\sum_{j=1}^{N_q} \|Rp_i + t - q_j\|^2$ is used to transform Q to register with P is called as backward square distance. When $det(A)$ convergence to zero, the sum of forward square distance becomes zero but the sum of backward square distance will be larger and make the function as well-posed. Here affine transformation is found using the procedure adopted in original ICP algorithm. First, new bidirectional correspondence for $(k-1)^{th}$ affine transformation (R_{k-1}, t_{k-1}) is evaluated as,

$$c_k(i) = \underset{\substack{j\in\{1,2,...,N_q\} \\ i\in\{1,2,...,N_p\}}}{\arg\min} \|A_{k-1}p_i + t_{k-1} - q_j\|^2$$

$$d_k(j) = \underset{\substack{j\in\{1,2,...,N_p\} \\ i\in\{1,2,...,N_q\}}}{\arg\min} \|A_{k-1}p_i + t_{k-1} - q_j\|^2 \tag{4.27}$$

Then K^{th} affine transformation (A_k, t_k) is evaluated based on the bidirectional correspondence $\{i, C_k(i)\}_{i=1}^{N_p}$ and $\{j, d_k(j)\}_{j=1}^{N_q}$ as,

$$(A_k, t_k) = \underset{A,t}{\arg\min} \left(\sum_{i=1}^{N_p} \left\| A p_i + t - q_{c_k(i)} \right\|^2 + \sum_{j=1}^{N_q} \left\| A p_{d_k(j)} + t - q_j \right\|^2 \right) \qquad (4.28)$$

The robust affine ICP algorithm can be evaluated using k-d tree and following steps are carried out:

Let $N = N_p + N_q$, $U = \{u_r\}_r^N$ and $V = \{v_r\}_r^N$, where u_r and v_r are evaluated as,

$$
\begin{aligned}
u_r &= \begin{cases} p_r, 1 \le r \le N_p \\ p_{d_k(r), N_p+1 \le r \le N} \end{cases} \\
v_r &= \begin{cases} q_{c_k(r)}, 1 \le r \le N_p \\ q_{r-N_p, N_p+1 \le r \le N} \end{cases}
\end{aligned}
\qquad (4.29)
$$

Now using u_r and v_r in equation 4.26, we can have the following equation.

$$(A_k, t_k) = \underset{A,t}{\arg\min} \left(\sum_{r=1}^{N} \left\| A u_r + t - v_r \right\|^2 \right) \qquad (4.30)$$

4.3 Results and Discussion

To valiate the matching algorithm between partial-to-full fingerprint using dots and incipient ridges, and pores. We have used NIST special database 30 (SD30) [4] and Rural Indian Fingerprint Database [5] of IIIT Delhi for performance evaluation. All images in SD30 are taken in constrained environment and images in IIIT database are taken in unconstrained environment. The earlier database includes 72 ten-print cards from 36 users, 10 fingers per user and 2 impressions per finger, scanned at both 500ppi and 1000ppi. The latter includes each 150 fingerprint of right hand and left hand index fingerprint image of urban and rural people and 10 print per each individual. So the total number of print is 3000 $((75 \times 2 \times 10) + (75 \times 2 \times 10))$. For performance measure, two experiments have been conducted for each database. In the first experiment on SD30, the first impression of each fingerprint is divided into 16 non-overlapping block of size 350×350 and rest pixels on the boundary are discarded. Thus total number of genuine and impostor match are 5760 and 2067840

respectively. Similarly, in case of Rural Indian Fingerprint Database, the first image is divided into 12 non-overlapping block of size 150×150 and rest pixels are discarded at the boundary. Number of probe image is 3600(300×12). Total number of genuine and impostor match are 3600 and 1076400 respectively. In the above case, we are taking non-overlapped partial print for matching against full print assuming that the matching is a partial to full matching. However, above case is not true in case of live data. For that we have randomly cropped 10 partial prints from the first impression and match them against second full impression. The total number of genuine and impostor scores are 3600 and 1292400 in case of NIST database, and 3000 and 897000 number for IIIT Delhi Fingerprint database respectively.

We have carried out two experiments: first experiment has been done using BOZORTH3 of NIST Biometric Image Software (NBIS) [39], a commercial software for matching, and the second experiment have been carried out based on our proposed matching technique using Delaunay triangulation described in Section 4.1. Figure 4.3 (I) and Figure 4.3 (II) shows the acceptance rate using BOZORTH3 [39] and using our proposed matching technique respectively in SD30 database. Similar experiment has been carried out using IIIT Delhi database and is shown in Figure 4.4 (I) and 4.4 (II) respectively. Another experiment has been carried using dots, incipient ridges and pores. In this experiment, match score based fusion has been employed. Matching score generated from Delaunay triangle based matching and RAICP based matching are fused using sum rule. Performance of the matching algorithm has been shown in Figure 4.5 and Figure 4.6 in NIST SD30 and IIIT Delhi database respectively.

The result has been shown using only level 2 feature and level 2 along with level 3 feature with both NIST SD30 database and IIIT Delhi Rural database. Accuracy of proposed method has been compared with Yi Chen [35] method in Table 4.1 and 4.2 using BOZORTH3 and proposed matching technique respectively. In [35], the partial print have been cropped manually. However, in our case, we have divided a full print into non-overlapped partial print. This method ensures that a partial print contains a region from all parts of a full fingerprint. Our method shows superiority over Yi Chen [35] method.

Table 4.1: Accuracy comparison of proposed extracted feature with BOZORTH3 matching with Yi Chen's approach for level 2 and level 2 with level 3 features using SD 30 and IIIT Delhi database.

Database	Proposed Approach				Chen Approach [35]			
	Non-Overlapped		Random Cropping		Manual Cropping		Random Cropping	
	level 2 Feature	Level 2 + 3 Feature	Level 2 Feature	Level 2+3 Feature	Level 2 Feature	Level 2 +3 Feature	Level 2 Feature	Level 2 +3 Feature
NIST SD30	82	88	85	90	82	87	85	90
IIIT Delhi	81	86	84	86	79	85	82	85

Table 4.2: Accuracy comparison of proposed extracted feature and proposed matching with Yi Chen's approach for level 2 and level 2 with level 3 features using SD 30 and IIIT Delhi database.

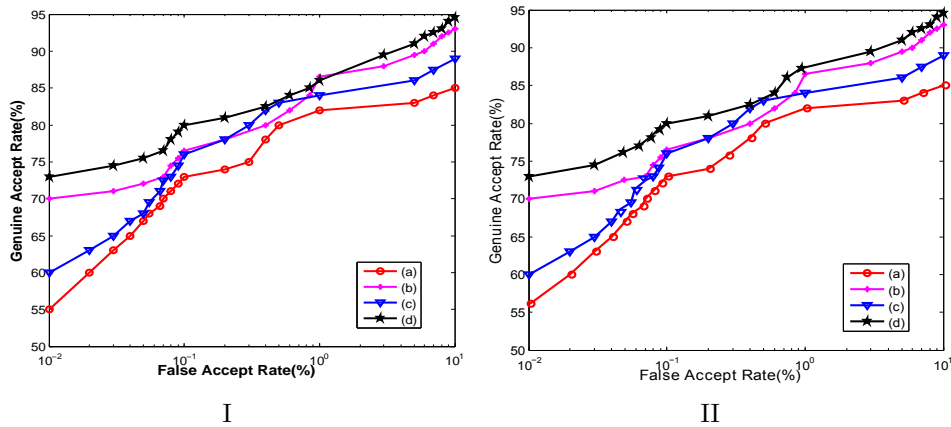| Database	Proposed Approach				Chen Approach [35]			
	Non-Overlapped		Random Cropping		Manual Cropping		Random Cropping	
	level 2 Feature	Level 2 + 3 Feature	Level 2 Feature	Level 2+3 Feature	Level 2 Feature	Level 2 +3 Feature	Level 2 Feature	Level 2 +3 Feature
NIST SD30	83	91	86	92	82	87	85	90
IIIT Delhi	82	89	84	90	79	85	82	85

Figure 4.3: ROC using SD 30 database (a) non-overlapped cropping using only level 2 features, (b) non-overlapped cropping using level 2 and level 3 features, (c) random cropping using only level 2 features, (d) random cropping using level 2 and level 3 features
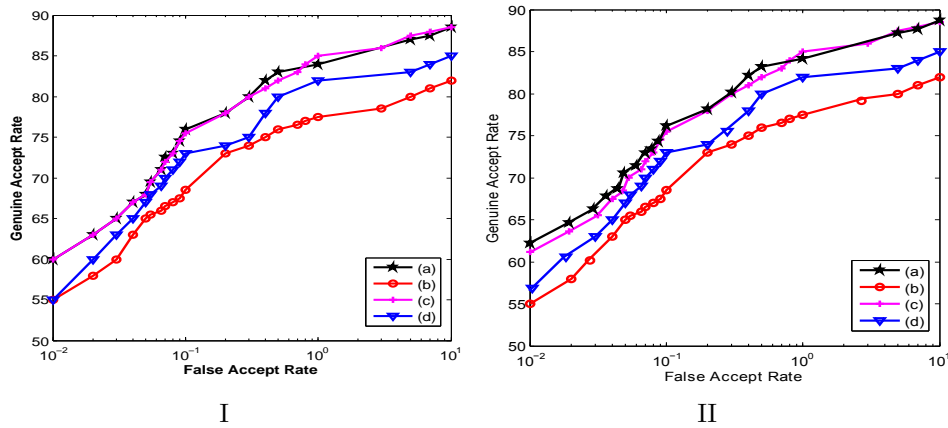

Figure 4.4: ROC using IIIT Delhi database (a) random cropping using level 2 and level 3 features, (b) non-overlapped cropping using only level 2 features, (c) non-overlapped cropping using level 2 and level 3 features, (d) random cropping using only level 2 features

4.4 Summary

In this chapter, one novel approach for fingerprint matching has been proposed. Both level 2 and level 3 features are used in Delaunay triangulation based matching. New set of feature vector are designed by connecting dots to the neighboring minutiae. Sum rule has been applied for fusing level 2 and level 3 matching score. For a comparative study, pore based matching has been described using a robust affine iterative closest point algorithm. As the experiment is a full-to-partial matching, partial print has been cropped in two ways: non-overlapped and random cropping. For non-overlapped
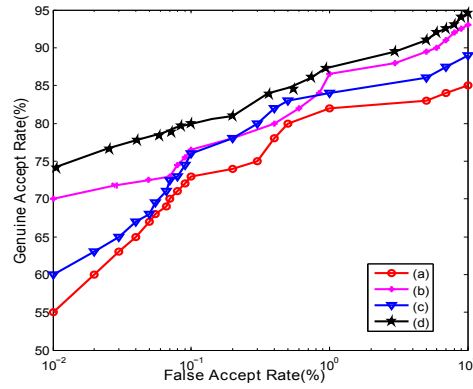
Figure 4.5: ROC using SD 30 database (a) non-overlapped cropping using only level 2 features, (b) non-overlapped cropping using level 2 and level 3 features, (c) random cropping using only level 2 features, (d) random cropping using level 2 and level 3 features
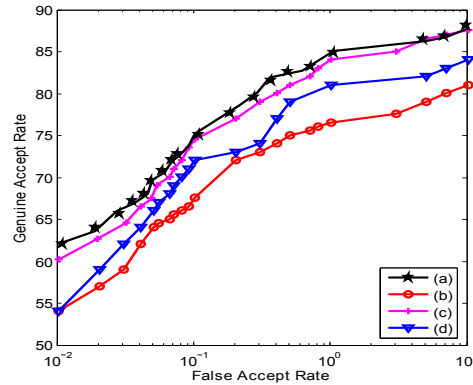

Figure 4.6: ROC using IIIT Delhi database (a) random cropping using level 2 and level 3 features, (b) non-overlapped cropping using only level 2 features, (c) non-overlapped cropping using level 2 and level 3 features, (d) random cropping using only level 2 features

cropping, BOZORTH3 and proposed matching technique is showing an accuracy of 88% and 91% respectively over NIST SD30 database. Similarly, for random cropping, accuracy for the mentioned matching scheme is 90% and 92% respectively over the same database. Another experiment has also been carried out over IIIT Delhi database. For non-overlapped cropping, BOZORTH3 and proposed matching technique is showing an accuracy of 86% and 89% respectively. For random cropping, the accuracy is 86% and 90% respectively. Another experiment has been performed using pores along with dots and incipient ridges. Pores are matched using RAICP algorithm. Delaunay triangle based matching score and RAICP based matching score are fused using *sum rule*. Over NIST SD30 database, for non-overlapped cropping

Table 4.3: Accuracy table of sum rule based fusion of RAICP and Delaunay triangle based matching score on SD 30 and IIIT Delhi database.

Database	Non-Overlapped		Random Cropping	
	Level 2 Feature	Level 2+ 3 Feature	Level 2 Feature	Level 2+3 Feature
NIST SD30	83	93	86	95
IIIT Delhi	82	94	84	92

and random cropping algorithm is showing an accuracy of 93% and 95% respectively. However, over IIIT Delhi database, for non-overlapped cropping and random cropping algorithm is showing an accuracy of 94% and 92% respectively.

Chapter 5

Conclusions and Future Work

This thesis proposes novel feature extraction and identification scheme for fingerprint. The first contribution is made on extraction of dots and incipient ridges. The extraction technique consists of three steps: 1) starting points have been found on valley by analyzing X-signature of a window taken from middle of the fingerprint, 2) valley has been traced using Fast Marching Method, 3) intensity based checking has been made for finding dots and incipient ridges. While matching, extracted features are added along with level 2 feature. The second contribution deals with matching of fingerprint using level 2 and level 3 features. Delaunay triangle has been constructed using level 2 feature. A novel algorithm of selecting compatible triangle pair is proposed. Level 2 feature based matching has been done using Delaunay triangle. New set of feature vectors are designed by connecting dots-and-incipients to the neighboring minutiae. Dots and incipient ridges based matching have been proposed using those feature parameters.

For a comparative study, pore based matching has been described using a robust affine iterative closest point algorithm. For performance evaluation of the proposed algorithm, two public database have been used: NIST SD30 database and IIIT Delhi rural database. Full-to-partial fingerprint matching has been done. Partial print is constructed by cropping a window from a full fingerprint in two ways: non-overlapped and random cropping. In the first experiment, dots and incipient ridges added with level 2 feature and matching have been done using BOZORTH3 of NBIS. Over NIST SD30 database, the accuracy is 88% and 90% for non-overlapped and random cropping respectively. Whereas, over IIIT Delhi database, accuracy

is 86% for both non-overlapped and random cropping. In the second experiment, proposed matching technique is used. Matching score of dots-and-incipients and level 2 feature are fused using *sum rule*. Over NIST SD30 database, the accuracy is 91% and 92% for non-overlapped and random cropping respectively. Where as, over IIIT Delhi database, accuracy is 89% and 90% for both non-overlapped and random cropping respectively. In the third experiment, matching score of dots-and-incipients, pores, and level 2 feature are fused using sum rule. Over NIST SD30 database, for non-overlapped cropping and random cropping, algorithm is showing an accuracy of 93% and 95% respectively. However, over IIIT Delhi database, for non-overlapped cropping and random cropping algorithm is showing an accuracy of 94% and 92% respectively. The research findings made out of this thesis have opened several research directions, which have a scope for further investigations. Sum rule has been employed for fusing level 2 and level 3 feature. However, a decision level fusion and kernel based fusion technique may show good results.

Bibliography

[1] A. K. Jain and D. Maltoni, *Handbook of Fingerprint Recognition.* Springer-Verlag New York, 2003.

[2] A. K. Jain, P. Flynn, and A. A. Ross, *Handbook of biometrics.* Springer, 2007.

[3] D. Maltoni, D. Maio, A. K. Jain, and S. Prabhakar, *Handbook of fingerprint recognition.* springer, 2009.

[4] C. Watson, "NIST special database 30: Dual resolution images from paired fingerprint cards," *National Institute of Standards and Technology, Gaithersburg*, 2001.

[5] C. Puri, K. Narang, A. Tiwari, M. Vatsa, and R. Singh, "On analysis of rural and urban indian fingerprint images," in *Ethics and Policy of Biometrics.* Springer, 2010, pp. 55–61.

[6] L. C. Henry and G. E. Robert, *Advances in fingerprint technology.* Elsevier Science, 2001.

[7] T. Reed and R. J. Meier, *Taking dermatoglyphic prints: a self-instruction manual.* American Dermatoglyphics Association, 1990.

[8] L. Henry and G. E. Robert, *Advances in fingerprint technology.* Elsevier Science, 2001.

[9] M. Hase and A. Shimisu, "Enrty method of fingerrpint imageusing a prism," *Transactions of the Institute of Electronics and Communication Engineers of Japan*, vol. J67-D, pp. 627–628, 1990.

[10] R. Bahuguna and T. Corboline, "Prism fingerprint sensor that uses a holographic optical element," *Applied optics*, vol. 35, no. 26, pp. 5242–5245, 1996.

[11] I. Seigo, E. Shine, and S. Takashi, "Holographic fingerprint sensor," *Fujitsu Scientific and Technical Journal*, vol. 35, pp. 287–287, 1989.

[12] W. S. Chen and C.-L. Kuo, "Apparatus for imaging fingerprint or topographic relief pattern on the surface of an object." Google Patents, 1995, US Patent 5,448,649.

[13] I. Fujieda, Y. Ono, and S. Sugama, "Fingerprint image input device having an image sensor with openings," 1995, US Patent 5,446,290.

[14] N. Young, G. Harkin, R. Bunn, D. McCulloch, R. Wilks, and A. Knapp, "Novel fingerprint scanning arrays using polysilicon TFT's on glass and polymer substrates," *IEEE Electron Device Letters*, vol. 18, no. 1, pp. 19–20, 1997.

[15] C. Tsikos, "Capacitive fingerprint sensor," 1982, US Patent 4,353,056.

[16] D. G. Edwards, "Fingerprint sensor," 1984, US Patent 4,429,413.

[17] L. O'Gorman and J. V. Nickerson, "Matched filter design for fingerprint image enhancement," in *International Conference on Acoustics, Speech, and Signal Processing (ICASSP)*. IEEE, 1988, pp. 916–919.

[18] L. O Gorman and J. V. Nickerson, "An approach to fingerprint filter design," *Pattern recognition*, vol. 22, no. 1, pp. 29–38, 1989.

[19] B. Sherlock, D. Monro, and K. Millard, "Fingerprint enhancement by directional fourier filtering," vol. 141, no. 2, pp. 87–94, 1994.

[20] L. Hong, Y. Wan, and A. Jain, "Fingerprint image enhancement: algorithm and performance evaluation," *IEEE Transactions on Pattern Analysis and Machine Intelligence*, vol. 20, no. 8, pp. 777–789, 1998.

[21] S. Greenberg, M. Aladjem, D. Kogan, and I. Dimitrov, "Fingerprint image enhancement using filtering techniques," in *15th International Conference on Pattern Recognition (ICPR)*, vol. 3. IEEE, 2000, pp. 322–325.

[22] E. NikodemuszSzekely and V. Szekely, "Image recognition problems of fingerprint identification," *Microprocessors and Microsystems.*, vol. 17, no. 4, pp. 215–218, 1993.

[23] M. Leung, W. Engeler, and P. Frank, "Fingerprint image processing using neural networks," in *10th Conference on Computer and Communication Systems*. IEEE, 1990, pp. 582–586.

[24] W. Leung, S. Leung, W. Lau, and A. Luk, "Fingerprint recognition using neural network," in *Proceedings of the 1991 IEEE Workshop on Neural Networks for Signal Processing*. IEEE, 1991, pp. 226–235.

[25] D. Maio and D. Maltoni, "Direct gray-scale minutiae detection in fingerprints," *IEEE Transactions on Pattern Analysis and Machine Intelligence*, vol. 19, no. 1, pp. 27–40, 1997.

[26] X. Jiang, W. Y. Yau, and W. Ser, "Minutiae extraction by adaptive tracing the gray level ridge of the fingerprint image," in *International Conference on Image Processing*, vol. 2. IEEE, 1999, pp. 852–856.

[27] J. Liu, Z. Huang, and K. L. Chan, "Direct minutiae extraction from gray-level fingerprint image by relationship examination," in *International Conference on Image Processing*, vol. 2. IEEE, 2000, pp. 427–430.

[28] K. Nilsson and J. Bigun, "Using linear symmetry features as a pre-processing step for fingerprint images," in *Audio-and Video-Based Biometric Person Authentication.* Springer, 2001, pp. 247–252.

[29] M. Ray, P. Meenen, and R. Adhami, "A novel approach to fingerprint pore extraction," in *Proceedings of the Thirty-Seventh Southeastern Symposium on System Theory.* IEEE, 2005, pp. 282–286.

[30] A. K. Jain, Y. Chen, and M. Demirkus, "Pores and ridges: Fingerprint matching using level 3 features," in *18th International Conference on Pattern Recognition (ICPR)*, vol. 4. IEEE, 2006, pp. 477–480.

[31] A. K. Jain and Y. Chen, "Pores and ridges: high-resolution fingerprint matching using level 3 features," *IEEE Transactions on Pattern Analysis and Machine Intelligence*, vol. 29, no. 1, pp. 15–27, 2007.

[32] Q. Zhao, D. Zhang, N. Luo, and J. Bao, "Adaptive pore model for fingerprint pore extraction," in *19th International Conference on Pattern Recognition (ICPR).* IEEE, 2008, pp. 1–4.

[33] S. Malathi, S. U. Maheswari, and C. Meena, "Fingerprint pore extraction based on marker controlled watershed segmentation," in *2nd International Conference on Computer and Automation Engineering (ICCAE)*, vol. 3. IEEE, 2010, pp. 337–340.

[34] N. Manivanan, S. Memon, and W. Balachandran, "Automatic detection of active sweat pores of fingerprint using highpass and correlation filtering," *Electronics letters.*, vol. 46, no. 18, pp. 1268–1269, 2010.

[35] Y. Chen and A. K. Jain, "Dots and incipients: extended features for partial fingerprint matching," in *Biometrics Symposium, 2007.* IEEE, 2007, pp. 1–6.

[36] K. Choi, H. Choi, S. Lee, and J. Kim, "Fingerprint image mosaicking by recursive ridge mapping," *IEEE Transactions on Systems, Man, and Cybernetics, Part B: Cybernetics,*, vol. 37, no. 5, pp. 1191–1203, 2007.

[37] D. R. Ashbaugh and C. Press, *Quantitative-qualitative friction ridge analysis: an introduction to basic and advanced ridgeology.* CRC press Boca Raton, 1999.

[38] B. M. Mehtre, "Fingerprint image analysis for automatic identification," *Machine Vision and Applications*, vol. 6, no. 2-3, pp. 124–139, 1993.

[39] C. I. Watson, M. D. Garris, E. Tabassi, C. L. Wilson, R. M. Mccabe, S. Janet, and K. Ko, "User's guide to NIST biometric image software (NBIS)," 2007.

[40] M. Indovina, V. Dvornychenko, R. Hicklin, and G. Kiebuzinski, "ELFT-EFS Evaluation of latent fingerprint technologies: Extended feature sets [evaluation# 2]," *National Institute of Standards and Technology, US Department of Commerce NISTIR*, vol. 7775, 2011.

[41] M. Rumpf and A. Telea, "A continuous skeletonization method based on level sets," in *Proceedings of the symposium on Data Visualisation 2002*. Eurographics Association, 2002, pp. 151–158.

[42] J. A. Sethian, "A fast marching level set method for monotonically advancing fronts," vol. 93, no. 4. National Academy Sciences, 1996, pp. 1591–1595.

[43] D. Arpit and A. Namboodiri, "Fingerprint feature extraction from gray scale images by ridge tracing," in *International Joint Conference on Biometrics (IJCB)*. IEEE, 2011, pp. 1–8.

[44] C. S. Burrus, R. A. Gopinath, H. Guo, J. E. Odegard, and I. W. Selesnick, *Introduction to wavelets and wavelet transforms: a primer*. Prentice hall New Jersey, 1998, vol. 23.

[45] T. Kanade and M. Okutomi, "A stereo matching algorithm with an adaptive window: Theory and experiment," *IEEE Transactions on Pattern Analysis and Machine Intelligence*, vol. 16, no. 9, pp. 920–932, 1994.

[46] J.-D. Zheng, Y. Gao, and M.-Z. Zhang, "Fingerprint matching algorithm based on similar vector triangle," in *2nd International Congress on Image and Signal Processing (CISP)*. IEEE, 2009, pp. 1–6.

[47] N. Liu, Y. Yin, and H. Zhang, "A fingerprint matching algorithm based on Delaunay triangulation net," in *The Fifth International Conference on Computer and Information Technology (CIT)*. IEEE, 2005, pp. 591–595.

[48] P. J. Besl and N. D. McKay, "Method for registration of 3-D shapes," in *Robotics-DL tentative*. International Society for Optics and Photonics, 1992, pp. 586–606.

[49] J. Zhu, S. Du, Z. Yuan, Y. Liu, and L. Ma, "Robust affine iterative closest point algorithm with bidirectional distance," *IET computer vision*, vol. 6, no. 3, pp. 252–261, 2012.

Dissemination

1. **Satyabrata Swain**, Banshidhar Majhi, and Ratnakar Dash, "Extended Feature Extraction Technique From Fingerprint," *Annual India Conference (INDICON), IEEE, 2014, Pune.* doi: 10.1109/INDICON.2014.7030491

2. **Satyabrata Swain**, Banshidhar Majhi, Ratnakar Dash, and Pankaj Kumar Sa, "Dots and Incipient based Fingerprint Matching Scheme using FMM and Delaunay Triangulation," *9th IEEE International Conference on Industrial and Information System (ICIIS), 2014, Gwalior.* doi: 10.1109/ICIINFS.2014.7036500

Satyabrata Swain

Computer Science and Engineering Department,
National Institute of Technology Rourkela,
Rourkela – 769 008, India.

+91 9124665185.

satya.swain10@gmail.com

Qualification

- M.Tech. (Research) (CSE) (Continuing)
  National Institute of Technology Rourkela.

- MCA
  Utkal University, Banivihar, [79.9%]

- B.Sc
  Ravenshaw University, Cuttack, [73.6%]

- 12th
  Kendrapara College, [72.2%]

- 10th
  Dashineswar High School, Kathiapara, [71.6%]

Permanent Address

AT – Minjauni
Po – Barapara
Dist – Kendrapara
State – Odisha Pin – 754245 (India)

Date of Birth

July 10, 1987